



# Phytoplankton Competition for Nutrients and Light in a Stratified Lake: A Mathematical Model Connecting Epilimnion and Hypolimnion

Jimin Zhang<sup>1</sup> · Jude D. Kong<sup>2</sup> · Junping Shi<sup>3</sup> · Hao Wang<sup>4</sup>

Received: 1 September 2020 / Accepted: 24 February 2021

© The Author(s), under exclusive licence to Springer Science+Business Media, LLC, part of Springer Nature 2021

## Abstract

A mathematical model connecting epilimnion and hypolimnion is proposed to describe the competition of phytoplankton for nutrients and light in a stratified lake. The existence and stability of nonnegative steady-state solutions are completely characterized for all possible parameter ranges by means of stability analysis, bifurcation theory, and extensive simulations. The critical thresholds for settling speed of phytoplankton cells in the thermocline and the loss rate of phytoplankton are established, which determine the survival or extirpation of phytoplankton in epilimnion and hypolimnion. In particular, it is shown that in two extreme cases, the principle of competitive exclusion always holds in a stratified lake. We also consider the influence of environmental parameters on the vertical distribution and biomass density of phytoplankton via a systematic sensitivity analysis, and investigate their roles in phytoplankton blooms. These results can be used for the prediction of phytoplankton competition and blooms in a stratified lake.

---

Communicated by Mary Silber.

---

Partially supported by NSFC-11971088, NSFHLJ-LH2019A022, NSF-DMS-1853598, and NSERC Discovery Grant RGPIN-2020-03911 and Accelerator Grant RGPAS-2020-00090.

---

✉ Junping Shi  
jxshix@wm.edu

<sup>1</sup> School of Mathematical Sciences, Heilongjiang University, Harbin 150080, Heilongjiang, People's Republic of China

<sup>2</sup> Department of Mathematics and Statistics, York University, North York, Toronto, ON M3J 1P3, Canada

<sup>3</sup> Department of Mathematics, William & Mary, Williamsburg, VA 23187-8795, USA

<sup>4</sup> Department of Mathematical and Statistical Sciences, University of Alberta, Edmonton, AB T6G 2G1, Canada

**Keywords** Reaction–diffusion model · Epilimnion · Hypolimnion · Nutrients · Light · Phytoplankton blooms · Principle of competitive exclusion

**Mathematics Subject Classification** 92D25 · 35K57 · 35B35 · 35B32 · 35B30

## 1 Introduction

Lakes are an important part of global water resources. They have special functions of regulating regional climate, recording regional environmental changes, protecting biodiversity, and recreation. Most deep lakes on Earth are stratified (Boehrer and Schultze 2008). Stratification separates the lake with a horizontal plane called thermocline into two zones : epilimnion and hypolimnion (Boehrer and Schultze 2008). The epilimnion is the upper zone which is warm (lighter) and well mixed. The hypolimnion is the bottom colder zone which is usually dark and relatively undisturbed.

Phytoplankton are the primary producer and the basis of energy flow and material circulation of the whole aquatic ecosystem. The growth of phytoplankton depends on two essential resources: nutrients and light. In oligotrophic aquatic ecosystems with ample supply of light, phytoplankton compete only for nutrients (Hsu et al. 2013; Nie et al. 2019; Wang et al. 2015; Zhang et al. 2018). In eutrophic ecosystems with ample nutrient supply, phytoplankton compete only for light (Du and Hsu 2010; Hsu and Lou 2010; Jiang et al. 2019; Peng and Zhao 2016). In some aquatic environments, phytoplankton compete for nutrients and light simultaneously (Du and Hsu 2008a; Mei and Zhang 2012; Ryabov et al. 2010; Yoshiyama and Nakajima 2002; Zagaris and Doelman 2011). Because the hypolimnion is not well mixed, the change in the phytoplankton density and nutrient concentration in it depends on time and depth in the water column. Phytoplankton can be moved from their position by turbulent mixing (diffusion) or by sinking (advection). The change in the phytoplankton density in the epilimnion is independent of the depth (since it is well mixed overnight).

Phytoplankton in epilimnion and hypolimnion compete for nutrients and light. Light from water surface first passes through epilimnion and then enters hypolimnion. This means that phytoplankton in epilimnion can absorb more light, and control the growth of phytoplankton in hypolimnion by shading. In contrast, nutrients from the benthos of the lake reach the epilimnion via the hypolimnion. As a consequence, phytoplankton in the hypolimnion have a dominant advantage for nutrients over their epilimnion counterparts. By reducing the nutrients input from hypolimnion to epilimnion, phytoplankton in the hypolimnion suppress the growth of epilimnion phytoplankton. Therefore, phytoplankton in epilimnion and hypolimnion form a spatially asymmetric competition for nutrients and light.

Due to the difficulty of measuring phytoplankton biomass, mathematical modeling of phytoplankton population is an important alternative method of improving our knowledge of the physical and biological processes relating to phytoplankton ecology (Edwards and Brindley 1999). Various mathematical models have been developed to examine phytoplankton competition for nutrients and light in a well-mixed surface layer (Wang et al. 2007; Alijani et al. 2015; Song et al. 2019; Jiang et al. 2019; Heggerud et al. 2020) and a poorly mixed deep layer (Hsu and Lou 2010; Du and Hsu

2008a; Yoshiyama et al. 2009; Du and Hsu 2008b; Klausmeier and Litchman 2001). To our knowledge, none of these models couple both the well-mixed and poorly mixed layers. However, to better understanding phytoplankton competition for nutrients and light in a stratified water column, it is essential to couple the dynamics of both layers. This can effectively be achieved using a hybrid of highly interconnected nonlinear partial and ordinary differential equations. Here we formulate and analyze a mathematical model of phytoplankton competition for nutrients and light in a stratified water column that couples both the well-mixed and poorly mixed layers. Using the model, we characterize all possibilities for the survival and extinction of phytoplankton in epilimnion and hypolimnion under the asymmetric competition mechanism between the epilimnion and hypolimnion phytoplankton. In particular, we show that in two extreme cases, the principle of competitive exclusion always holds no matter what the value of phytoplankton loss rate is. The mathematical model of phytoplankton and nutrients in epilimnion and hypolimnion (see (2.1)) that we propose here is a hybrid system of two ordinary differential equations and two diffusive partial differential equations with nonlocal terms, and the exchanges of phytoplankton and nutrients through the interface between epilimnion and hypolimnion make the system a coupled ODE-PDE system which is also called bulk-surface or bulk-membrane system. Such systems couple the boundary ODE and interior PDE through the boundary condition, and they appeared frequently in the study of cell polarization models (Cusceddu et al. 2019; Gomez et al. 2019; Paquin-Lefebvre et al. 2020a, b). Mathematical analysis of these systems is a newly emerging challenge, and we develop some new techniques in stability analysis which may be useful for other similar problems.

The vertical distribution and biomass density of phytoplankton are two important indices in evaluating phytoplankton blooms and protecting water quality (Yoshiyama et al. 2009; Huisman et al. 2006; Jäger et al. 2010; Klausmeier and Litchman 2001; Vasconcelos et al. 2016). Phytoplankton are highly heterogeneous in vertical spatial distribution and exhibit the phenomenon of vertical aggregation in poorly mixed water columns (Du and Hsu 2008a; Ryabov et al. 2010; Yoshiyama and Nakajima 2002; Du and Hsu 2008b; Klausmeier and Litchman 2001). This vertical aggregation is influenced by biological and abiotic factors, and the aggregation layer is constantly changing. In particular, when phytoplankton gather in the epilimnion of the lake, it is easy to induce the occurrence of phytoplankton blooms. The surge of phytoplankton biomass is an important manifestation of phytoplankton blooms, which seriously damages the water quality and leads to the death of a large number of aquatic organisms. Another objective of this present paper is to explore the influence of environmental parameters on the vertical distribution and biomass density of phytoplankton and investigate their roles in phytoplankton blooms.

The rest of the paper is organized as follows. In Sect. 2, we derive a mathematical model to describe the competition of phytoplankton for nutrients and light in the epilimnion and hypolimnion. We then investigate the existence and stability of all non-negative steady-state solutions for this model by using stability analysis and bifurcation theory in Sect. 3. In Sect. 4, according to realistic environmental parameters, we use some numerical simulations to illustrate and supplement theoretical analysis, and give a complete characterization for the distribution region of steady-state solutions based on settling speed of phytoplankton cells in the thermocline and the loss rate of

phytoplankton. In Sect. 5, we consider the influence of environmental parameters on the vertical distribution and biomass density of phytoplankton, and it indicates their roles in phytoplankton blooms. Finally, we summarize our findings and state some questions for future study in Sect. 6.

## 2 Derivation of the Model

We propose a mathematical model of epilimnion and hypolimnion ecosystem to describe the interactions of phytoplankton, nutrients (i.e., phosphorus or nitrogen) and light in a stratified lake. Let  $x$  denote the depth coordinate of the lake. The epilimnion as a completely mixed layer is located in the upper layer of the lake and is assumed to have depth  $x_e$ . The hypolimnion, the poorly mixed layer, is located in the lower part of the lake and has depth  $x_h$ . There is a seasonal zone called thermocline between them, and its thickness is very thin compared to the maximum depth of the lake. Hence, we ignore the thickness of the thermocline in our model. Let  $x = -x_e$  be the surface of the lake, let  $x = 0$  be the interface between epilimnion and hypolimnion, and let  $x = x_h$  be the bottom of hypolimnion, see Fig. 1.

Phytoplankton and nutrients are divided into two parts: biomass density  $A(t)$  of phytoplankton and concentration  $N(t)$  of dissolved nutrients in epilimnion, and biomass density  $B(x, t)$  of phytoplankton and concentration  $M(x, t)$  of dissolved nutrients in hypolimnion with  $0 \leq x \leq x_h$ . The growth of phytoplankton is assumed to depend on two resources: light intensity  $I$  and nutrients  $N, M$ . The light intensity at each depth  $x$  of the lake is described by the Lambert–Beer law (Huisman and Weissing 1994) as

$$I(x, A) = I_{in} \exp(-K_{bg}(x + x_e) - I(x + x_e)A), \quad -x_e \leq x \leq 0,$$

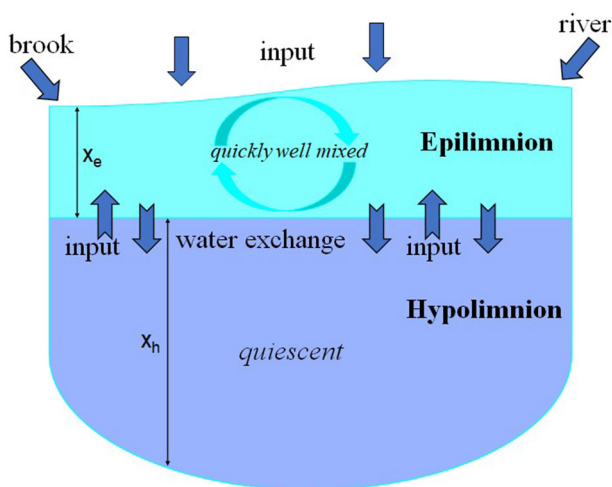


Fig. 1 Epilimnion and hypolimnion ecosystem in a stratified lake. Adapted from Wang et al. (2007)

in epilimnion and

$$I(x, A, B) = I_{in} \exp\left(-K_{bg}(x + x_e) - lx_e A - l \int_0^x B(z)dz\right), \quad 0 \leq x \leq x_h,$$

in hypolimnion.

From Yoshiyama and Nakajima (2002), Etemad-Shahidi and Imberger (2001), Wüest and Lorke (2003), the thermocline between epilimnion and hypolimnion is a non-turbulent layer. The diffusive transport of nutrients across the thermocline is vertical diffusion with Brownian motion. While the diffusive transport of phytoplankton across the thermocline is much smaller (almost negligible) than that of nutrients. Therefore, in this paper we assume that phytoplankton exchange between epilimnion and hypolimnion is only affected by buoyancy and gravity of phytoplankton cells and nutrient exchange between them is dominated by Brownian motion. In the non-turbulent layer, phytoplankton will sink since the density of phytoplankton protoplasm is generally higher than that of water. Phytoplankton have a mechanism to self-regulate their sinking speed, such as the production of gas vesicle and the storage of lipids with lower density, so that they stay in the bright zone for a longer time and get a greater growth chance. We denote  $a$  to be the settling speed of phytoplankton cells in the thermocline, and  $b$  be the diffusion rate of nutrients/exchange rate (caused by Brownian motion in the thermocline).

The epilimnion is usually well mixed because of its large turbulent diffusion effect (Yoshiyama and Nakajima 2002; Huisman and Weissing 1994). Therefore, here we assume that phytoplankton and dissolved nutrients in epilimnion are spatially uniformly distributed. The intrinsic growth rate of phytoplankton depends on the light density  $I(x, A)$  and nutrients  $N(t)$ . Define Monod functions:

$$f(N) = \frac{N}{N + \gamma_1}, \quad g(I) = \frac{I}{I + \gamma_2}.$$

Then, the phytoplankton intrinsic growth rate is proportional to the product of  $f(N)$  and the average light intensity  $g(I)$  in the epilimnion:

$$f(N) \frac{1}{x_e} \int_{-x_e}^0 g(I(x, A))dx = f(N) \frac{1}{x_e(K_{bg} + lA)} \ln \frac{I_{in} + \gamma_2}{I_{in} \exp(-x_e(K_{bg} + lA)) + \gamma_2}.$$

This form of multiplication of two resource functions has been used in previous studies (see Wang et al. 2007; Zagaris and Doelman 2011; Alijani et al. 2015; Heggerud et al. 2020). The other commonly used algebraic form for modeling two irreplaceable resources is the minimum value of two resource functions  $\min\{f(N), g(I)\}$  based on Liebig's law of the minimum (see for example, Du and Hsu 2008a, b; Klausmeier and Litchman 2001). The two functions are qualitatively similar in the sense that  $f \cdot g \leq \min\{f, g\} \leq \sqrt{f \cdot g}$  as  $0 \leq f, g \leq 1$  while the value of the multiplicative function is smaller than the one of the minimum functions. Here we use the product form as it is a differentiable function which is more mathematically convenient. As a result of death, respiration and predation, the biomass density of phytoplankton in

epilimnion is lost at a density-independent rate  $\delta$ . Phytoplankton sinking takes place at the interface between epilimnion and hypolimnion, and its rate is negatively related to the volume of epilimnion, because with a larger volume there is relatively less proportion of total species abundances or element concentrations for sinking. The change of the nutrients  $N(t)$  in epilimnion is due to consumption by phytoplankton with the nutrients to carbon quota  $\theta$ , nutrient recycling from the loss of phytoplankton with proportion  $p \in [0, 1]$  and nutrient exchange between epilimnion and hypolimnion with the exchange rate  $b$ .

The hypolimnion is a poorly mixed layer (Yoshiyama and Nakajima 2002; Wüest and Lorke 2003). Let  $B(x, t)$  and  $M(x, t)$  denote the biomass density of phytoplankton and concentration of dissolved nutrients at depth  $x \in [0, x_h]$  and time  $t$  in hypolimnion, respectively. Phytoplankton transport in hypolimnion is governed by random movement owing to turbulence with a diffusion coefficient  $D_b$  and directional movement due to gravity with a speed  $v$ . The intrinsic growth rate of phytoplankton in hypolimnion also depends on the light density  $I(x, A, B)$  and nutrients  $M(x, t)$  in the multiplicative form of  $f(M)g(I(x, A, B))$ . The biomass density of phytoplankton is lost at the rate  $\delta$ . There is a phytoplankton input from epilimnion at  $x = 0$  and a no-flux boundary condition at  $x = x_h$ . The change of dissolved nutrients  $M(x, t)$  in hypolimnion depends on turbulent diffusion with a diffusion coefficient  $D_m$ , consumption by phytoplankton, nutrient recycling from the loss of phytoplankton biomass. There is a nutrient exchange between epilimnion and hypolimnion at  $x = 0$  and a fixed nutrient input  $M_b$  at  $x = x_h$ .

According to the above discussions, we have the following phytoplankton-light-nutrients model in epilimnion and hypolimnion, which is a hybrid system of two ordinary differential equations and two partial differential equations with nonlocal terms. All the variables and parameters of the model and their biological meanings are listed in Table 1.

$$\left\{ \begin{array}{ll} \frac{dA}{dt} = rAf(N)\frac{1}{x_e} \int_{-x_e}^0 g(I(x, A))dx - \frac{a}{x_e}A - \delta A, & t > 0, \\ \frac{dN}{dt} = \frac{b}{x_e}(M(0, t) - N) + \theta p\delta A - \theta rAf(N)\frac{1}{x_e} \int_{-x_e}^0 g(I(x, A))dx, & t > 0, \\ \frac{\partial B}{\partial t} = D_b \frac{\partial^2 B}{\partial x^2} - v \frac{\partial B}{\partial x} + rBf(M)g(I(x, A, B)) - \delta B, & 0 < x < x_h, t > 0, \\ \frac{\partial M}{\partial t} = D_m \frac{\partial^2 M}{\partial x^2} + \theta p\delta B - \theta rBf(M)g(I(x, A, B)), & 0 < x < x_h, t > 0, \\ D_b \frac{\partial B(0, t)}{\partial x} - vB(0, t) = -aA, D_b \frac{\partial B(x_h, t)}{\partial x} - vB(x_h, t) = 0, & t > 0, \\ D_m \frac{\partial M(0, t)}{\partial x} = b(M(0, t) - N(t)), M(x_h, t) = M_b, & t > 0, \\ I(x, A) = I_{in} \exp(-K_{bg}(x + x_e) - l(x + x_e)A), & -x_e \leq x \leq 0, \\ I(x, A, B) = I_{in} \exp\left(-K_{bg}(x + x_e) - x_e l A - l \int_0^x B(z, t) dz\right), & 0 < x < x_h. \end{array} \right. \quad (2.1)$$

Here we assume that  $v \in \mathbb{R}$ ,  $a \geq 0$ ,  $0 \leq p \leq 1$  and the remaining parameters are all positive constants. Considering the biological meaning of model (2.1), we will deal

**Table 1** Variables and parameters of model (2.1) with biological meanings

Symbol	Meaning	Symbol	Meaning
$t$	Time	$x$	Depth
$x_e$	Depth of epilimnion	$x_h$	Depth of hypolimnion
$A$	Biomass density of phytoplankton in epilimnion	$N$	Concentration of dissolved nutrients in epilimnion
$B$	Biomass density of phytoplankton in hypolimnion	$M$	Concentration of dissolved nutrients in hypolimnion
$D_b, D_m$	Vertical turbulent diffusivity of phytoplankton and dissolved nutrients in hypolimnion, respectively	$v$	Sinking or buoyant velocity of phytoplankton in hypolimnion
$r$	Maximum specific production rate of phytoplankton	$I_{in}$	Light intensity at the water surface
$K_{bg}$	Background light attenuation coefficient	$\delta$	Loss rate of phytoplankton
$l$	Light attenuation coefficient of phytoplankton	$\theta$	Average cell quota of phytoplankton
$p$	Proportion of nutrients in phytoplankton losses that is recycled	$\gamma_1$	Half-saturation constant for light-limited production of phytoplankton
$\gamma_2$	Half saturation constant for nutrient-limited production of phytoplankton	$b$	Nutrient exchange rate between epilimnion and hypolimnion
$a$	Settling speed of phytoplankton cells in the thermocline	$M_b$	Concentration of dissolved nutrients at the bottom of hypolimnion

with the solutions of (2.1) with nonnegative initial values, i.e.,

$$A(0) = A_0 > 0, \quad N(0) = N_0 > 0, \quad B(x, 0) = B_0(x) \geq \neq 0, \quad M(x, 0) = M_0(x) \geq \neq 0.$$

Model (2.1) is a very complex system. It contains nonlocal terms and the coupling of ODE and PDE through boundary conditions, which makes it extremely challenging to analyze the dynamic properties of the system. In order to clarify phytoplankton competition in a stratified lake, we will analyze steady-state solutions of model (2.1) in the next section by using the stability analysis and bifurcation theory.

### 3 Existence and Stability of Steady States

In this section, we investigate the existence and stability of nonnegative steady state solutions of (2.1). A steady state  $E = (A, N, B(x), M(x))$  is a semi-trivial one if at least one component of  $E$  is zero, and it is a coexistence steady state if each component is positive.

### 3.1 Semi-Trivial Steady States

This subsection focuses on the existence and stability of semi-trivial steady state solutions of (2.1). The possible nonnegative semi-trivial steady states of (2.1) are listed below:

1. Nutrient-only semi-trivial steady state  $E_1 : (0, N_1^*, 0, M_1^*(x))$ , where  $N_1^*$  and  $M_1^*(x)$  satisfy

$$\begin{cases} M(0) - N = 0, \\ M''(x) = 0, \quad 0 < x < x_h, \\ D_m M'(0) = b(M(0) - N), \quad M(x_h) = M_b; \end{cases} \tag{3.1}$$

2. Phytoplankton in epilimnion semi-trivial steady state  $E_2 : (A_2^*, N_2^*, 0, M_2^*(x))$  for  $a = 0$ , where  $A_2^*, N_2^*$  and  $M_2^*(x)$  satisfy

$$\begin{cases} rf(N) \frac{1}{x_e} \int_{-x_e}^0 g(I(x, A)) dx - \delta = 0, \\ \frac{b}{x_e} (M(0) - N) + \theta(p - 1)\delta A = 0, \\ M''(x) = 0, \quad 0 < x < x_h, \\ D_m M'(0) = b(M(0) - N), \quad M(x_h) = M_b; \end{cases} \tag{3.2}$$

3. Phytoplankton in hypolimnion semi-trivial steady state  $E_3 : (0, N_3^*, B_3^*(x), M_3^*(x))$ , where  $N_3^*, B_3^*(x)$  and  $M_3^*(x)$  satisfy

$$\begin{cases} M(0) - N = 0, \\ D_b B''(x) - vB'(x) + rBf(M)g(I(x, 0, B)) - \delta B = 0, \quad 0 < x < x_h, \\ D_m M''(x) + \theta p \delta B - \theta r Bf(M)g(I(x, 0, B)) = 0, \quad 0 < x < x_h, \\ D_b B'(0) - vB(0) = D_b B'(x_h) - vB(x_h) = 0, \\ D_m M'(0) = b(M(0) - N), \quad M(x_h) = M_b. \end{cases} \tag{3.3}$$

In the following we discuss the existence, uniqueness and stability of each type of semi-trivial steady-state solutions listed above for different loss rate  $\delta$  and settling speed  $a$ , and also discuss the implication of such steady states to the whole dynamics of (2.1).

For the convenience of the following discussion, for any given  $D > 0, v \geq 0$  and  $q \in L^\infty([0, x_h])$ , we denote  $\lambda_1(D, v, q(x))$  to be the principal eigenvalue of eigenvalue problem

$$\begin{cases} D\phi''(x) - v\phi'(x) + q(x)\phi = \lambda\phi, & x \in (0, x_h), \\ D\phi'(0) - v\phi(0) = D\phi'(x_h) - v\phi(x_h) = 0. \end{cases} \tag{3.4}$$

From Proposition 3.1 in Wang et al. (2019), the principal eigenvalue  $\lambda_1(D, v, q(x))$  of (3.4) exists and it is unique, and  $\lambda_1(D, v, q_1(x)) \geq \lambda_1(D, v, q_2(x))$  if  $q_1(x) \geq q_2(x)$ . We define the following critical death rates:

$$\begin{aligned} \delta_0^* &= f(M_b) \frac{r}{x_e} \int_{-x_e}^0 g(I(x, 0)) dx, \quad \delta_a^* = \delta_0^* - \frac{a}{x_e}, \\ \delta_* &= \lambda_1(D_b, v, rf(M_b)g(I(x, 0, 0))), \\ \delta_a^{**} &= \frac{r}{x_e} \int_{-x_e}^0 g(I(x, 0)) dx - \frac{a}{x_e}, \quad \delta_{**} = \lambda_1(D_b, v, rg(I(0, 0, 0))). \end{aligned} \tag{3.5}$$

The thresholds  $\delta_0^*, \delta_a^*$ , respectively, represent the intrinsic growth rate of the epilimnion phytoplankton when its growth depends only on the nutrients from the hypolimnion and the average light intensity on  $[-x_e, 0]$  (that is independent of the total biomass above it). Observe that if there is no turbulent upward transport of nutrients to the photic zone,  $\delta_0^* = 0$  and  $\delta_a^* = -a/x_e$ . Turbulent upward transport of nutrients to the photic zone is usually the most strongly limiting process in deep waters. A direct calculation gives

$$\begin{aligned} \frac{1}{x_e} \int_{-x_e}^0 g(I(z, A)) dz &> g(I(x, A, B)) \text{ for any } x \in [0, x_h], A, B \geq 0, \\ \delta_a^* &> \delta_* \text{ if } 0 \leq a < x_e(\delta_0^* - \delta_*), \text{ and } \delta_* > \delta_a^* \text{ if } a > x_e(\delta_0^* - \delta_*). \end{aligned}$$

In the following discussion, it is shown that  $\delta_a^*$  and  $\delta_*$  are two threshold loss rates for phytoplankton to invade aquatic ecosystems.

For any parameter value, (2.1) always has a unique nutrient-only semi-trivial steady state  $E_1$ , and it is also stable if the phytoplankton loss rate is high. The following result precisely determines the stability of  $E_1$  in terms of the loss rate  $\delta$ . The proof is given in ‘‘Appendix A.’’

**Theorem 3.1** *System (2.1) has a unique nutrients-only semi-trivial steady-state solution  $E_1 \equiv (0, M_b, 0, M_b)$ . If*

$$\delta > \max \{ \delta_a^*, \delta_* \}, \tag{3.6}$$

*then  $E_1$  is locally asymptotically stable with respect to (2.1), while  $E_1$  is unstable if*

$$\delta < \max \{ \delta_a^*, \delta_* \}. \tag{3.7}$$

*Moreover, if*

$$\delta > \max \{ \delta_a^{**}, \delta_{**} \}, \tag{3.8}$$

*then  $E_1$  is globally asymptotically stable for (2.1) with respect to any nonnegative initial value.*

**Remark 3.2** The condition (3.6) shows that the large phytoplankton loss rate in epilimnion and hypolimnion causes extinction of phytoplankton and the existence of only nutrients. This means that  $\max\{\delta_a^*, \delta_*\}$  is a critical value for phytoplankton to invade a stratified lake. The condition (3.8) implies that in this case, phytoplankton extinction is inevitable for all initial conditions. The threshold  $\delta_a^{**}$  represents the light dependent per capita growth rate of phytoplankton assuming that the light intensity reaching each phytoplankton in the epilimnion is independent of the phytoplankton biomass above it. The threshold  $\delta_{**}$  represents the light intensity dependent per capita growth rate of phytoplankton in the thermocline. Phytoplankton biomass is lost via excretion, respiration or grazing. Thus, if grazing is high,  $E_1$  will be stable. Also, if either the turbulent upward transport of nutrients to the photic zone or light intensity is low,  $E_1$  will be locally asymptotically stable. This means that high nutrient input concentration and light intensity are conducive to phytoplankton invasion.

From an intuitive point of view, if the sinking speed  $a$  is not zero and not very large, the existence of phytoplankton in epilimnion will certainly lead to the existence of phytoplankton in hypolimnion, and both will coexist in the stratified lake. If the sinking speed  $a$  is greater than a certain threshold, only phytoplankton in hypolimnion will exist. Therefore, it can be seen that  $E_2$  exists only when the settling speed  $a$  of phytoplankton cells in the thermocline is zero. The following results show that  $\delta_0^*$  is a critical value for phytoplankton in epilimnion to invade the aquatic ecosystem, and the proof is given in “Appendix A.”

**Theorem 3.3** Assume that  $a = 0$  and  $p \in [0, 1]$ . Then

(i) System (2.1) has a unique positive phytoplankton in epilimnion semi-trivial steady state

$$E_2 \equiv (A_2^*, N_2^*, 0, M_2^*(x)) \\ = \left( A_2^*, M_b - \left( \frac{x_h}{D_m} + \frac{1}{b} \right) (1-p)\theta\delta x_e A_2^*, 0, M_b - \frac{x_h - x}{D_m} (1-p)\theta\delta x_e A_2^* \right)$$

if and only if

$$0 < \delta < \delta_0^*, \quad (3.9)$$

where  $A_2^*$  satisfies

$$f(N_2^*) \frac{r}{x_e} \int_{-x_e}^0 g(I(x, A_2^*)) dx = \delta; \quad (3.10)$$

(ii) If in addition to (3.9), we also have

$$\delta > \lambda_1 (D_b, v, rf(M_2^*)g(I(x, A_2^*, 0))), \quad (3.11)$$

then  $E_2$  is locally asymptotically stable with respect to (2.1), while  $E_2$  is unstable if

$$\delta < \lambda_1 (D_b, v, rf(M_2^*)g(I(x, A_2^*, 0))) . \tag{3.12}$$

In particular, there exists  $\epsilon > 0$  such that  $E_2$  is locally asymptotically stable with respect to (2.1) if  $\delta_0^* - \epsilon < \delta < \delta_0^*$ . Moreover when  $p = 1$ ,  $E_2$  is locally asymptotically stable with respect to (2.1) if  $0 < \delta < \delta_0^*$ .

- Remark 3.4**
1. The condition (3.9) indicates that  $\delta_0^*$  is a critical value for phytoplankton in epilimnion to invade a stratified lake. If the condition (3.11) also holds, then phytoplankton in epilimnion win the competition, that is, the stratified lake has most phytoplankton in the top layer. When phytoplankton mainly concentrate in epilimnion, phytoplankton blooms can very likely occur.
  2. When  $p = 1$ , nutrients in dead phytoplankton are completely recycled back to media, then phytoplankton in epilimnion have more nutrients to use and thus become a stronger competitor than phytoplankton in hypolimnion. Numerical simulations indicate that  $E_2$  is globally asymptotically stable for (2.1) in this situation. This shows that the competition exclusion principle also holds for this extreme case.
  3. When  $0 \leq p < 1$ , numerical simulations suggest that there exists a positive  $\delta_0^{***} < \delta_0^*$  such that  $E_2$  is unstable and a coexistence steady state exists for  $0 < \delta < \delta_0^{***}$ . This critical death rate  $\delta_0^{***}$  is a threshold value for phytoplankton in hypolimnion to invade the aquatic ecosystem in this situation, and phytoplankton in epilimnion and hypolimnion coexist in the stratified lake when  $0 < \delta < \delta_0^{***}$  and  $a = 0$ .
  4. From (3.5), the threshold death rate  $\delta_0^* = \delta_0^*(M_b, I_{in}, x_e)$  depends on the nutrient input concentration  $M_b$ , the light intensity  $I_{in}$  and the depth of epilimnion  $x_e$ . One can observe that  $\delta_0^*$  is strictly increasing with respect to  $M_b$  and  $I_{in}$ . Hence for any fixed  $\delta \in (0, \delta_0^{**})$ , there exists a unique critical nutrient input concentration  $M_b^{**} > 0$  such that  $\delta = \delta_0^*(M_b^{**}, I_{in}, x_e)$ , and similarly for any fixed  $\delta > 0$  there exists a unique critical light intensity  $I_{in}^{**} > 0$  such that  $\delta = \delta_0^*(M_b, I_{in}^{**}, x_e)$ . When  $M_b > M_b^{**}$  or  $I_{in} > I_{in}^{**}$ , phytoplankton in epilimnion persist; and when  $0 < M_b < M_b^{**}$  or  $0 < I_{in} < I_{in}^{**}$ , phytoplankton in epilimnion will be extirpated. Note that

$$\frac{d\delta_0^*}{dx_e} = \frac{rf(M_b)}{x_e K_{bg}} \left( g(I(0, 0)) - \frac{1}{x_e} \int_{-x_e}^0 g(I(x, 0))dx \right) < 0,$$

which implies that  $\delta_0^*$  is strictly decreasing with respect to  $x_e$ . This means that there is a unique critical epilimnion depth  $x_e^{**} > 0$  such that  $\delta = \delta_0^*(M_b, I_{in}, x_e^{**})$ . Phytoplankton in epilimnion persist if  $0 < x_e < x_e^{**}$ , and phytoplankton in epilimnion become extirpated if  $x_e > x_e^{**}$ . Similar observations also hold for  $\delta_a^* = \delta_a^*(M_b, I_{in}, x_e)$  with respect to  $M_b$  and  $I_{in}$ .

Next we show the existence of phytoplankton in hypolimnion semi-trivial steady state  $E_3$  when  $a > x_e(\delta_0^* - \delta_*)$  by using bifurcation theory with  $\delta$  as the bifurcation parameter. In this case, for the two threshold death rates  $\delta_a^*$  and  $\delta_*$ , we have  $\delta_* > \delta_a^*$ ;

thus, phytoplankton in epilimnion can invade the stratified lake but phytoplankton in hypolimnion cannot. A solution  $E_3$  for a given parameter value  $\delta$  is in a form of  $(\delta, N, B(x), M(x))$ , where  $\delta, N > 0, B \in X_1$ , and  $M \in X_2$  where

$$\begin{aligned} X_1 &:= \{u \in C^2([0, x_h]) : D_b u'(0) - vu(0) = D_b u'(x_h) - vu(x_h) = 0\}, \\ X_2 &:= C^2([0, x_h]). \end{aligned} \tag{3.13}$$

Define  $\Lambda$  to be the set of all positive solutions  $(\delta, N, B, M) \in (\mathbb{R}^+)^2 \times X_1 \times X_2$  of (3.3). The existence of  $E_3$  is as follows and the proof is given in ‘‘Appendix A.’’

**Theorem 3.5** *Assume that  $a > x_e(\delta_0^* - \delta_*)$  (i.e.,  $\delta_* > \delta_a^*$ ) holds. Then*

- (i) *System (2.1) has at least one positive phytoplankton in hypolimnion semi-trivial steady state solution  $E_3$  (with  $A = 0$ ) for  $0 < \delta < \delta_*$ ;*
- (ii) *There exists a connected component  $\Lambda^+$  of  $\Lambda$  such that the closure of  $\Lambda^+$  contains the bifurcation point  $(\delta_*, M_b, 0, M_b)$  where  $\Lambda^+$  connects to the line of nutrient-only solutions  $\Gamma_1 = \{(\delta, M_b, 0, M_b) : \delta > 0\}$ , and the projection of  $\Lambda^+$  onto  $\delta$ -axis contains the interval  $(0, \delta_*)$ ;*
- (iii) *Near  $(\delta_*, M_b, 0, M_b)$ ,  $\Lambda^+$  is a smooth curve in a form  $\{(\delta_3(s), N_3^*(s), B_3^*(s, x), M_3^*(s, x)) : 0 < s < \varepsilon_3\}$  for some  $\varepsilon_3 > 0$  with  $\delta_3'(0) < 0$ .*

**Remark 3.6** 1. Theorem 3.5 shows that  $E_3$  exists in  $(0, \delta_*)$ , and  $\delta_*$  is a critical value for the existence/nonexistence of phytoplankton in hypolimnion. For the stability of  $E_3$ , we cannot get any results from the theoretical analysis since (3.3) is a nonlocal predator-prey system. By using realistic environmental parameters, our numerical simulations show that if  $\delta_a^* < \delta < \delta_*$ , then all solutions of (2.1) converge to  $E_3$ . In this case, phytoplankton in hypolimnion win the competition and the stratified lake has most phytoplankton in the bottom layer. Moreover, when  $0 < \delta < \delta_a^*$  and  $x_e(\delta_0^* - \delta_*) < a < x_e \delta_0^*$ , phytoplankton in epilimnion and hypolimnion coexist in a stratified lake.

- 2. It can be seen from the first equation in (2.1) that if  $a > x_e \delta_0^*$ ,  $A \rightarrow 0$  as  $t \rightarrow \infty$  when  $N \leq M_b$ . Our numerical simulations also indicate that when  $a > x_e \delta_0^*$ ,  $E_3$  is globally asymptotically stable on  $(0, \delta_*)$ . This means that if the settling speed is large enough, then the competition exclusion principle holds and phytoplankton mainly concentrate in hypolimnion. The above results show that the settling speed of phytoplankton cells in the thermocline is beneficial to reduce the probability of phytoplankton blooms.
- 3. From (3.5), the threshold death rate  $\delta_* = \delta_*(M_b, I_{in}, x_h, D_b, v)$  depends on vertical turbulent diffusivity  $D_b$ , sinking/buoyant velocity  $v$ , the nutrient input concentration  $M_b$ , the light intensity  $I_{in}$  and the depth of hypolimnion  $x_h$ . It is clear that  $\delta_*$  is strictly increasing with respect to  $M_b$  and  $I_{in}$ . This implies that for fixed  $\delta$  there exist unique critical nutrient input concentration  $M_b^*$  (when  $\delta < \delta_{**}$ ) and critical light intensity  $I_{in}^*$  (when  $\delta > 0$ ) such that  $\delta = \delta_*(D_b, v, M_b^*, I_{in}, x_h)$  and  $\delta = \delta_*(D_b, v, M_b, I_{in}^*, x_h)$ , respectively; phytoplankton in hypolimnion persist if  $M_b > M_b^*$  (or  $I_{in} > I_{in}^*$ ), and phytoplankton in hypolimnion become extirpated if  $0 < M_b < M_b^*$  (or  $0 < I_{in} < I_{in}^*$ ). On the other hand, according to Theorems 3.2-3.9 in Hsu and Lou (2010),  $\delta_*$  is strictly decreasing in  $v$  and  $x_h$ , and there

exist unique critical sinking/buoyant velocity  $v^*$  and critical hypolimnion depth  $x_h^*$  such that  $\delta = \delta_*(D_b, v^*, M_b, I_{in}, x_h)$  and  $\delta = \delta_*(D_b, v, M_b, I_{in}, x_h^*)$  with persistence/extirpation threshold behavior. The dependence of  $\delta_*$  on  $D_b$  is more complicated, and there are possibly one or more critical turbulent diffusivity that affect the survival and extirpation of phytoplankton in hypolimnion.

### 3.2 Coexistence Steady States

A coexistence steady-state solution  $E_4 : (A_4^*, N_4^*, B_4^*(x), M_4^*(x))$  satisfies

$$\begin{cases} rf(N) \frac{1}{x_e} \int_{-x_e}^0 g(I(x, A)) dx - \delta - \frac{a}{x_e} = 0, \\ \frac{b}{x_e} (M(0) - N) + \left( \theta p \delta - \theta rf(N) \frac{1}{x_e} \int_{-x_e}^0 g(I(x, A)) dx \right) A = 0, \\ D_b B''(x) - v B'(x) + r B f(M) g(I(x, A, B)) - \delta B = 0, & 0 < x < x_h, \\ D_m M''(x) + (\theta p \delta - \theta rf(M) g(I(x, A, B))) B = 0, & 0 < x < x_h, \\ D_b B'(0) - v B(0) = -aA, \quad D_b B'(x_h) - v B(x_h) = 0, \\ D_m M'(0) = b(M(0) - N), \quad M(x_h) = M_b. \end{cases} \tag{3.14}$$

We now show the bifurcation of the coexistence steady state  $E_4$  from the nutrients-only semi-trivial steady state  $E_1$  at  $\delta = \delta_a^*$  for  $0 < a < x_e(\delta_0^* - \delta_*)$ . Note that a solution  $E_4$  for a given bifurcation parameter value  $\delta$  is in a form of  $(\delta, A, N, B(x), M(x))$ , where  $\delta, A, N > 0, B \in X_1$ , and  $M \in X_2$ . We define  $\Upsilon$  to be the set of all positive solutions  $(\delta, A, N, B, M) \in (\mathbb{R}^+)^3 \times X_1 \times X_2$  of (3.14).

**Theorem 3.7** *Assume that  $0 < a < x_e(\delta_0^* - \delta_*)$  (i.e.,  $\delta_* < \delta_a^*$ ). Then*

- (i) System (2.1) has at least one positive coexistence steady-state solution  $E_4$  for  $0 < \delta < \delta_a^*$ ;
- (ii) There exists a connected component  $\Upsilon^+$  of  $\Upsilon$  such that the closure of  $\Upsilon^+$  contains the bifurcation point  $(\delta_a^*, M_b, 0, M_b)$  where  $\Upsilon^+$  connects to the line of nutrient-only solutions  $\Gamma_1 = \{(\delta, M_b, 0, M_b) : \delta > 0\}$ , and the projection of  $\Upsilon^+$  onto  $\delta$ -axis contains the interval  $(0, \delta_a^*)$ ;
- (iii) Near  $(\delta_a^*, 0, M_b, 0, M_b)$ ,  $\Upsilon^+$  is a smooth curve in a form  $\{(\delta_4(s), A_4^*(s), N_4^*(s), B_4^*(s, x), M_4^*(s, x)) : 0 < s < \varepsilon_4\}$  for some  $\varepsilon_4 > 0$  with  $\delta_4'(0) < 0$ .

**Remark 3.8** 1. The above theorem shows that phytoplankton in epilimnion and hypolimnion can coexist in the stratified lake when  $0 < a < x_e(\delta_0^* - \delta_*)$ . From the perspective of competition, phytoplankton in epilimnion have a dominant advantage for light from the water surface, while phytoplankton in hypolimnion have a dominant advantage for nutrients from the sediment. This mechanism forms an asymmetric competition for light and nutrients, which leads to the coexistence of competitive populations to a certain extent.

2. Here we only establish the bifurcation of the coexistence steady-state  $E_4$  from  $E_1$  at  $\delta = \delta_a^*$  for  $0 < a < x_e(\delta_0^* - \delta_*)$ . In fact, our numerical simulations show that

$E_4$  can also bifurcate from  $E_2$  at  $\delta = \delta_0^{***}$  for  $a = 0$  and from  $E_3$  at  $\delta = \delta_a^*$  for  $x_e(\delta_0^* - \delta_*) < a < x_e\delta_0^*$ .

### 4 Simulations

To illustrate and supplement our above theoretical analysis, we do some numerical simulations according to the values of biologically reasonable parameters listed in Table 2. A detailed statement of the numerical methods is found in ‘‘Appendix B.’’

For the convenience of the following discussion, we take  $(\delta, a)$  as the parameters and divide the positive  $(\delta, a)$  quadrant into subregions as follows:

$$\begin{aligned}
 \Delta_{11} &:= \{(\delta, a) : \delta_0^* < \delta, a = 0\}, \\
 \Delta_{12} &:= \{(\delta, a) : \delta_a^* < \delta, 0 < a < x_e(\delta_0^* - \delta_*)\}, \\
 \Delta_{13} &:= \{(\delta, a) : \delta_* < \delta, x_e(\delta_0^* - \delta_*) < a\}, \\
 \Delta_{21} &:= \{(\delta, a) : 0 < \delta < \delta_0^*, a = 0, p = 1\}, \\
 \Delta_{22} &:= \{(\delta, a) : \delta_0^{***} < \delta < \delta_0^*, a = 0, p \in [0, 1)\}, \\
 \Delta_{31} &:= \{(\delta, a) : \delta_a^* < \delta < \delta_*, x_e(\delta_0^* - \delta_*) < a < x_e\delta_0^*\}, \\
 \Delta_{32} &:= \{(\delta, a) : 0 < \delta < \delta_*, x_e\delta_0^* < a\}, \\
 \Delta_{41} &:= \{(\delta, a) : 0 < \delta < \delta_0^{***}, a = 0, p \in [0, 1)\}, \\
 \Delta_{42} &:= \{(\delta, a) : 0 < \delta < \delta_a^*, 0 < a < x_e(\delta_0^* - \delta_*)\}, \\
 \Delta_{43} &:= \{(\delta, a) : 0 < \delta < \delta_a^*, x_e(\delta_0^* - \delta_*) < a < x_e\delta_0^*\}.
 \end{aligned}
 \tag{4.1}$$

A total extinction of the system will never occur because of the presence of the fixed external dissolved nutrients  $M_b$  at the bottom of hypolimnion. The extinction of phytoplankton in the epilimnion and hypolimnion can occur if the phytoplankton loss rate is very large (see Theorem 3.1 and  $\Delta_{1i}, i = 1, 2, 3$  in Figs. 2 and 3). If this happens, the concentration of dissolved nutrients in epilimnion and hypolimnion will both be the same as the concentration of dissolved nutrients  $M_b$  at the bottom of the hypolimnion. This means that in the absence of phytoplankton, dissolved nutrients in the epilimnion and hypolimnion are distributed evenly.

Phytoplankton and dissolved nutrients in the epilimnion can coexist in a stratified lake if the settling speed of phytoplankton cells in the thermocline is zero (see Theorem 3.3 and  $\Delta_{2i}, i = 1, 2$  in Fig. 2). If nutrients are completely recycling ( $p = 1$ ), then the phytoplankton in the epilimnion will be a stronger competitor compared to phytoplankton in hypolimnion. In this situation, the semi-trivial steady of epilimnion phytoplankton  $E_2$  exists and it is stable in  $\Delta_{21}$ , while the hypolimnion phytoplankton goes to extinction (see Theorem 3.3 and Figs. 2 and 4a). This means that the principle of competition exclusion holds in this extreme case, and it is likely to cause phytoplankton blooms. Another different scenario is when nutrients are only recycling partially ( $0 \leq p < 1$ ). In this situation, the parameter region where  $E_2$  exists and is stable is  $\Delta_{22}$  (see Theorem 3.3 and Figs. 2 and 4b). If the loss rate of phytoplank-

**Table 2** Numerical values of parameters of model (2.1) with references.

Symbol	Values	Units	Source	Symbol	Values	Units	Source
$x_e$	6	m	Assumption	$x_h$	6	m	Assumption
$D_b, D_m$	0.2 (0.1–10)	m <sup>2</sup> /day	Grover (2017), Huisman et al. (2002), Huisman et al. (2006), Jäger et al. (2010), Klausmeier and Litchman (2001), Ryabov et al. (2010)	$v$	0.1(-0.2–0.5)	m/day	Grover (2017), Huisman et al. (2002), Jäger and Diehl (2014), Jäger et al. (2010), Ryabov et al. (2010)
$r$	1	day <sup>-1</sup>	Jäger and Diehl (2014), Yoshiyama and Nakajima (2002)	$I_{in}$	400	μmol m <sup>-2</sup> s <sup>-1</sup>	Vasconcelos et al. (2016)
$K_{bg}$	0.25(0.1–1)	m <sup>-1</sup>	Jäger and Diehl (2014), Vasconcelos et al. (2016)	$\delta$	0.1	day <sup>-1</sup>	Jäger and Diehl (2014), Vasconcelos et al. (2016)
$l$	0.0003	m <sup>2</sup> /mg C	Vasconcelos et al. (2016)	$\theta$	0.008	mgP/mg C	Vasconcelos et al. (2016)
$p$	0.1 (0–1)	–	Assumption	$\gamma_1$	3	mg P/m <sup>3</sup>	Jäger and Diehl (2014), Vasconcelos et al. (2016)
$\gamma_2$	80	μmol m <sup>-2</sup> s <sup>-1</sup>	Vasconcelos et al. (2016)	$b$	0.864	m/day	Yoshiyama and Nakajima (2002)
$a$	0.1	m/day	Assumption	$M_b$	40	mg P/m <sup>-3</sup>	Ryabov et al. (2010), Yoshiyama and Nakajima (2002)

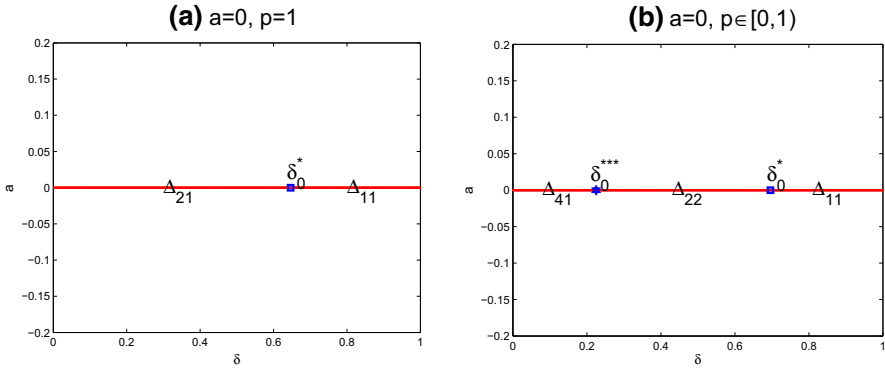


**Fig. 2** Parameter ranges in the  $\delta$ -line from extinction to existence of phytoplankton for  $a = 0$  as defined in (4.1). Other parameters are shown in Table 2

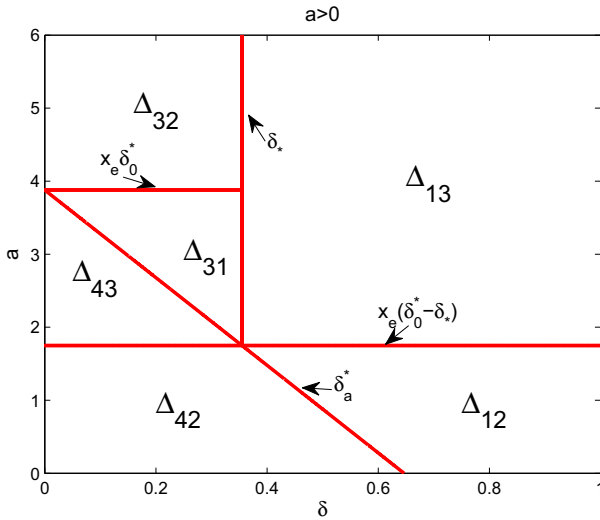


**Fig. 3** Parameter ranges in the  $(\delta, a)$ -plane from extinction to existence of phytoplankton as defined in (4.1). Other parameters are shown in Table 2

ton is further reduced, then  $E_2$  loses its stability, and phytoplankton exist in both the epilimnion and hypolimnion layers of the lake.

Phytoplankton and dissolved nutrients in hypolimnion can also coexist independently in a stratified lake if the settling speed of phytoplankton cells in the thermocline is large (see Theorem 3.5 and  $\Delta_{3i}$ ,  $i = 1, 2$  in Fig. 3). When  $x_e(\delta_0^* - \delta_*) < a < x_e\delta_0^*$ , the phytoplankton in hypolimnion semi-trivial steady state  $E_3$  exists and it is stable in  $\Delta_{31}$  (see Theorem 3.5 and Fig. 5b). The phytoplankton in hypolimnion control the growth of the phytoplankton in epilimnion by limiting nutrients from the water bottom. In particular, if the settling speed is large enough ( $a > x_e\delta_0^*$ ), the phytoplankton in epilimnion goes to extinction, and the phytoplankton concentrates only in the hypolimnion, which prevents the occurrence of phytoplankton blooms (see Fig. 5c).

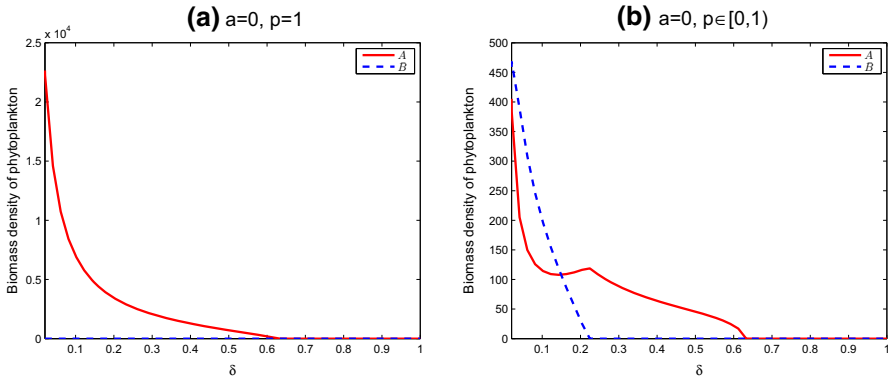


**Fig. 4** Bifurcation diagram of phytoplankton for  $a = 0$ . Here  $\bar{B} = (1/x_h) \int_0^{x_h} B(x)dx$  and other parameters are shown in Table 2

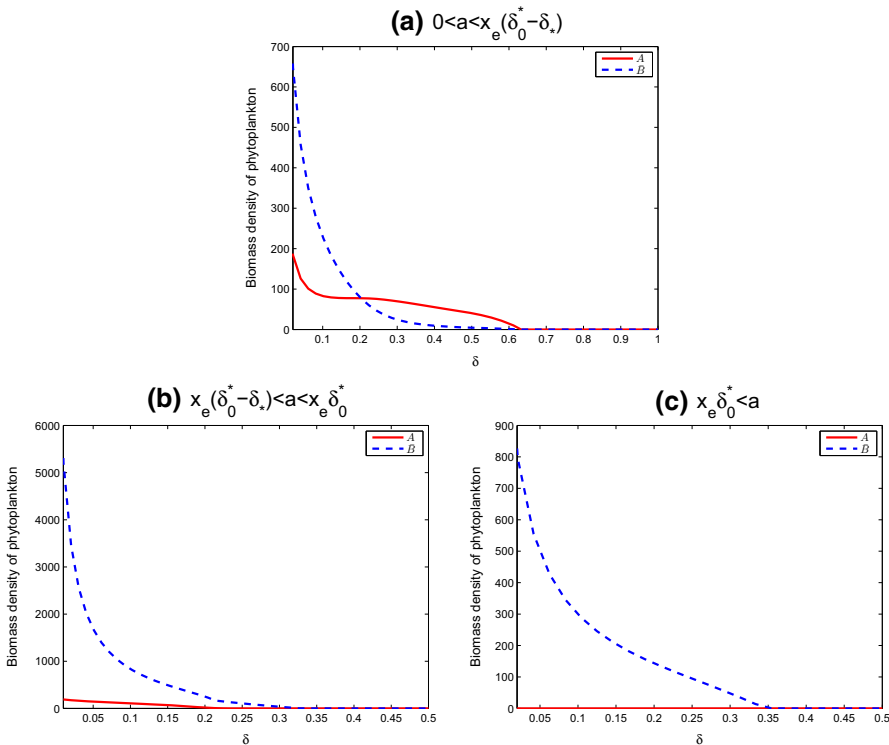


**Fig. 5** Bifurcation diagram of phytoplankton for  $\delta \in (0, 1)$ . Here  $\mathbf{a} = 0.1$ ,  $\mathbf{b} = 2.5$ ,  $\mathbf{c} = 4$  and other parameters are shown in Table 2

This also indicates that the settling speed of phytoplankton cells in the thermocline is an important parameter in the assessment of phytoplankton blooms.

Phytoplankton in epilimnion and hypolimnion can appear together in the stratified lake for three different cases. The first case is that if  $a = 0$  and  $p \in [0, 1)$ , then they coexist in  $\Delta_{41}$  (see Figs. 2 and 4b). The second case is that they appear together in  $\Delta_{42}$

**Table 3** Existence and local stability of steady states for model (2.1)

Regions	$E_1$	$E_2$	$E_3$	$E_4$
$\Delta_{1i} (i = 1, 2, 3)$	E(T) and S(T)	–	–	–
$\Delta_{2i} (i = 1, 2)$	E(T) and US(T)	E(T) and S(T)	–	–
$\Delta_{3i} (i = 1, 2)$	E(T) and US(T)	–	E(T) and S(N)	–
$\Delta_{41}$	E(T) and US(T)	E(T) and US(T)	–	E(N) and S(N)
$\Delta_{42}$	E(T) and US(T)	–	–	E(T) and S(N)
$\Delta_{43}$	E(T) and US(T)	–	E(T) and US(N)	E(N) and S(N)

*E* Existence, – non-existence, *S* locally stable, *US* unstable, *T* results of theoretical analysis, *N* results of numerical simulation

when  $0 < a < x_e(\delta_0^* - \delta_*)$  (see Theorem 3.7 and Figs. 3 and 5a). The third case is that they coexist in  $\Delta_{43}$  if  $x_e(\delta_0^* - \delta_*) < a < x_e\delta_0^*$  (see Figs. 3 and 5b). Light from the water surface and nutrients from the water bottom form an asymmetric resource supply mechanism for the phytoplankton growth. Phytoplankton in epilimnion located in the upper layer have a light dominance, while phytoplankton in hypolimnion located in the lower layer have a nutrient dominance. Hence phytoplankton in epilimnion and hypolimnion constitute an asymmetric competition for nutrients and light. This mechanism leads to the coexistence of phytoplankton in epilimnion and hypolimnion in the stratified lake.

From the above discussion, we identify threshold loss rates of phytoplankton  $\delta_0^*, \delta_a^*, \delta_*, \delta_0^{***}$  and threshold settling speeds of phytoplankton cells in the thermocline  $0, x_e(\delta_0^* - \delta_*), x_e\delta_0^*$ , which describe persistence and extinction of phytoplankton in epilimnion and hypolimnion. In particular, there are two extreme cases. One is that the settling speed rate is zero ( $a = 0$ ) and nutrients are completely recycling ( $p = 1$ ), and the other one is when the settling speed rate is large enough ( $a > x_e\delta_0^*$ ). In these two extreme cases, the principle of competitive exclusion always holds.

We summarize the results of the above theoretical analysis and numerical simulations on the existence and local stability of nonnegative steady-state solutions of model (2.1) shown in Table 3.

### 5 Phytoplankton Vertical Distribution and Density

The vertical distribution of phytoplankton biomass plays an important role in regulating an aquatic ecosystem. They can be significantly influenced by water movement and depth, light and nutrients. It is of great interest to evaluate the effects of these abiotic factors on the vertical distribution of phytoplankton. We observe that parameters in model (2.1) are closely related to these factors. For example, the spatial parameters  $D_b, D_m, v$  and depth  $x_e, x_h$  of epilimnion and hypolimnion are related to water movement and depth;  $I_{in}, K_{bg}, l$  and  $\gamma_2$  are related to light;  $M_b, p, \theta$  and  $\gamma_1$  are related to nutrients. Therefore, in this section, we investigate the influence of environmental parameters in model (2.1) on the vertical distribution and biomass density of phytoplankton in epilimnion and hypolimnion.

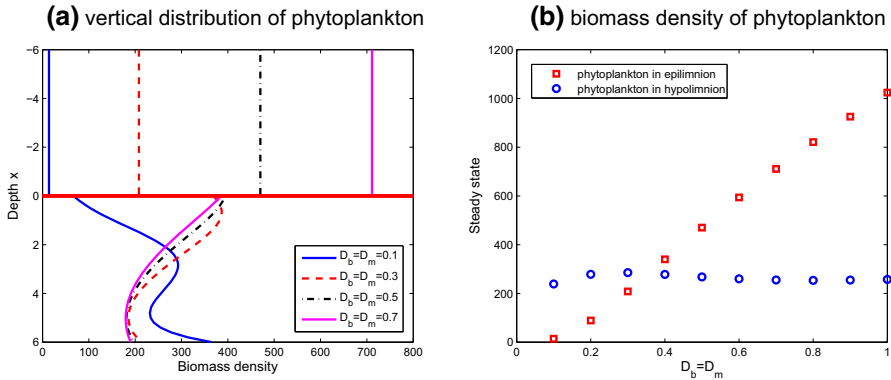


**Fig. 6** Influence of parameters  $D_b, D_m$  on the vertical distribution and biomass density of phytoplankton. The results show that high vertical turbulent diffusivity ( $D_b, D_m$ ) in the hypolimnion causes phytoplankton to accumulate in the epilimnion and the increase in the biomass density in the epilimnion. Here other parameters are shown in Table 2. The horizontal straight line at  $x = 0$  is the thermocline, above which is epilimnion and below which is hypolimnion

In order to facilitate the discussion below, we only consider the coexistence steady states  $A_4$  and  $B_4(x)$  and let the spatial average of  $B_4(x)$  be  $\bar{B}_4 = (1/x_h) \int_0^{x_h} B_4(x) dx$ . In figures below, the vertical distribution profiles for four different parameter choices are shown on the left, and the dependence of biomass densities on this parameter in the two lake layers is shown on the right. We will compare the coexistence steady-state biomass density  $A_4, \bar{B}_4$  and the coexistence steady-state vertical distribution  $A_4, B_4(x)$  for different parameter values.

We first consider the effect of spatial parameters  $D_b, D_m$  and  $v$  on the vertical distribution and biomass density of phytoplankton. Figure 6 shows the impact of the vertical turbulent diffusivity  $D_b, D_m$  on the vertical distribution and biomass density of phytoplankton. A high vertical turbulent diffusion causes phytoplankton populations to outgrow sinking. (see Fig. 6a). In this case, there is a biomass density regime shift from hypolimnion to epilimnion. The biomass density in the epilimnion surges, while the one in the hypolimnion has a slight change (see Fig. 6b). The reason for the above phenomenon is that with the increase in the turbulent diffusion, nutrients are more fully transmitted from the bottom to the top, so that phytoplankton in the epilimnion reduce their dependence on nutrients, which may lead to phytoplankton blooms. An interesting phenomenon here is that there are two phytoplankton accumulating layers in hypolimnion when  $D_b = D_m = 0.1$ . This indicates that there may be one or more maximum points for the phytoplankton biomass distribution, also regarded as an important indicator of Deep Chlorophyll Maxima (DCMs), in a lake as a result of the limitation of biological and abiotic factors.

Figure 7a shows that a transition of phytoplankton in the hypolimnion from floating to sinking, and it causes a change in the aggregation of phytoplankton from the top to the bottom of the hypolimnion. Meanwhile, the biomass density of phytoplankton in epilimnion and hypolimnion reveals a non-monotonic property. In the epilimnion, the biomass density first decreases and then increases, while in the hypolimnion, it

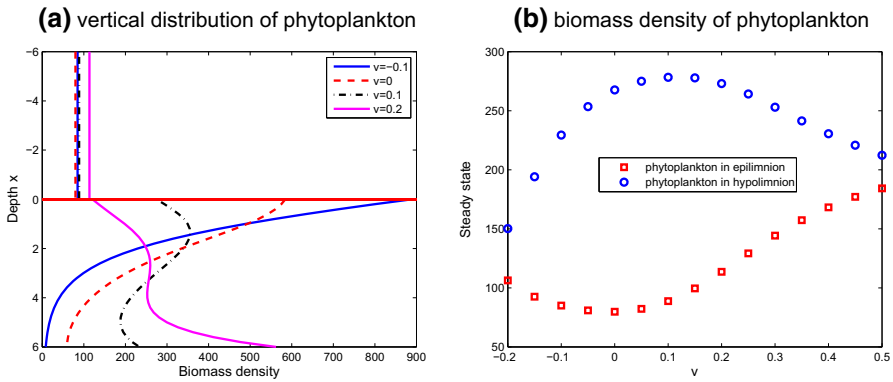


**Fig. 7** Influence of parameter  $v$  on the vertical distribution and biomass density of phytoplankton. The results indicate that  $v$  in hypolimnion has no obvious effect on phytoplankton blooms. Here other parameters are shown in Table 2

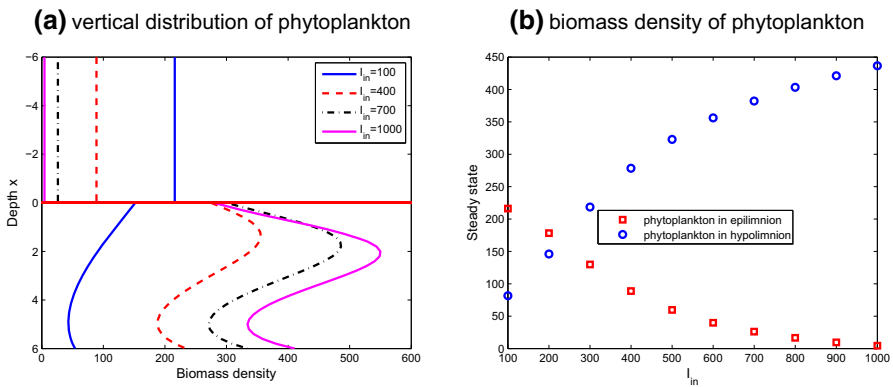


**Fig. 8** Influence of parameter  $I_{in}$  on the vertical distribution and biomass density of phytoplankton. The results show that high light intensity  $I_{in}$  can lead to phytoplankton aggregation and rapid increase in biomass in the hypolimnion. Here other parameters are shown in Table 2

is the opposite (see Fig. 7b). When phytoplankton in hypolimnion float up ( $v < 0$ ) due to phototaxis, they reduce the absorption of nutrients, which causes a reduction in the biomass density. While the biomass density of phytoplankton in epilimnion increases due to the reduction in competition. On the contrary, in the process of sinking ( $v > 0$ ), the biomass density of phytoplankton in hypolimnion decreases owing to the limitation of light. This leads to an increase in the biomass density of phytoplankton in epilimnion.

In Fig. 8, one can see that when the light intensity  $I_{in}$  is low, phytoplankton mainly gather in epilimnion, while when  $I_{in}$  is high, phytoplankton gather in hypolimnion. This is because, a high  $I_{in}$  implies that phytoplankton in epilimnion can not suppress the rapid growth of phytoplankton in hypolimnion. But phytoplankton in hypolimnion is still able to control the growth of phytoplankton in epilimnion through low nutrient concentration  $M_b$ . This suggests that phytoplankton in hypolimnion are a stronger

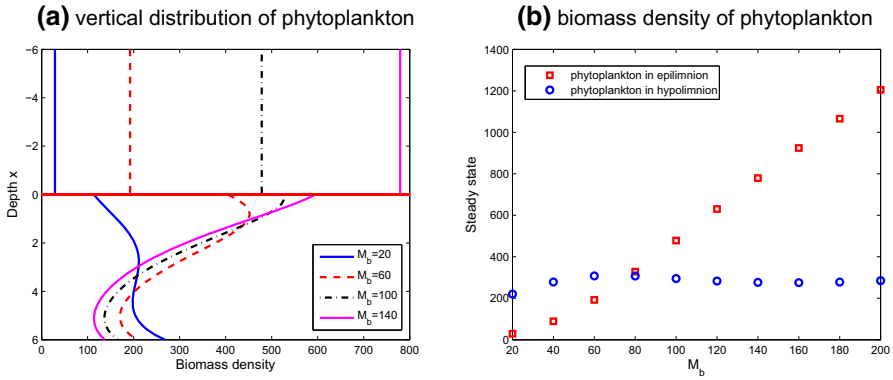


**Fig. 9** Influence of parameter  $M_b$  on the vertical distribution and biomass density of phytoplankton. The results show that high nutrient concentration  $M_b$  causes phytoplankton aggregation in the epilimnion, and is easy to induce phytoplankton blooms. Here other parameters are shown in Table 2

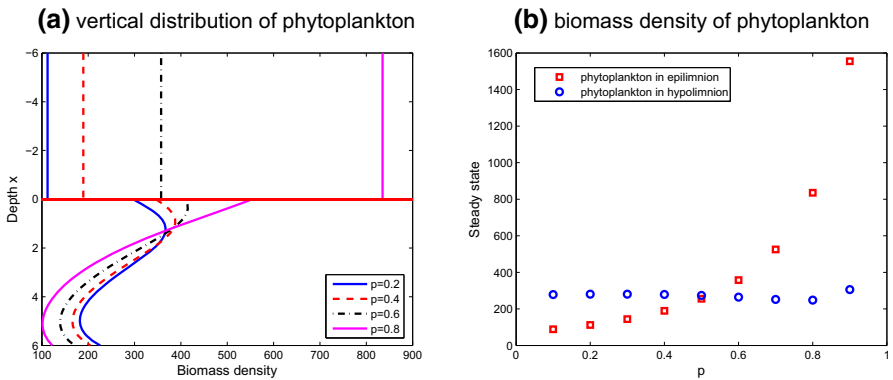


**Fig. 10** Influence of parameter  $p$  on the vertical distribution and biomass density of phytoplankton. The results show that if the nutrient recycling rate  $p$  is high enough, then even in oligotrophic aquatic ecosystems phytoplankton may bloom. Here other parameters are shown in Table 2

competitor in this asymmetric competition under high light intensity. On the other hand, if the nutrient concentration increases gradually, it produces an opposite result. Phytoplankton gather in the epilimnion, and phytoplankton in the epilimnion become a stronger competitor under high nutrient concentration and low light intensity (see Fig.9). It also confirms once again that phytoplankton blooms are more likely to occur in eutrophic lakes. It can be seen from the above discussion that under the asymmetric competition mechanism, if a resource that was initially limiting become abundant, the weaker competitor for the resource may win the competition.

In view of the increase in nutrient recycling proportion  $p$ , phytoplankton reduce the dependence on nutrients; thus, phytoplankton in hypolimnion cannot control the rapid growth of phytoplankton in the epilimnion through the asymmetric competition. However, phytoplankton in epilimnion as a stronger competitor is still able to suppress the growth of phytoplankton in hypolimnion through low light intensity. This results in

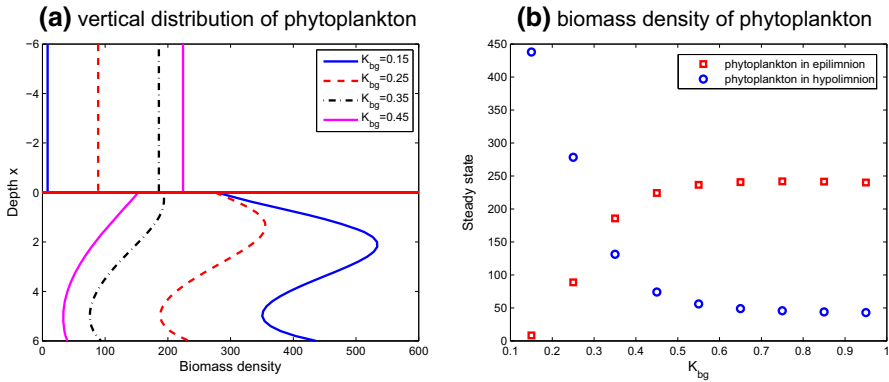


**Fig. 11** Influence of parameter  $K_{bg}$  on the vertical distribution and biomass density of phytoplankton. The results show that low light attenuation coefficient  $K_{bg}$  is beneficial to control phytoplankton blooms. Here other parameters are shown in Table 2

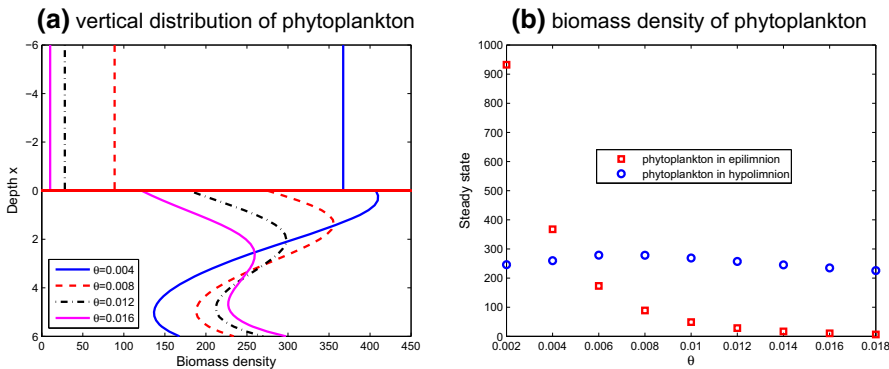


**Fig. 12** Influence of parameter  $\theta$  on the vertical distribution and biomass density of phytoplankton. The results indicate that with the increase in  $\theta$ , phytoplankton gather at the benthos and the biomass of the epilimnion decreases sharply. Here other parameters are shown in Table 2

a slight effect of  $p$  on the vertical distribution and biomass density of phytoplankton in hypolimnion and a great effect on the biomass density of phytoplankton in hypolimnion (see Fig. 10). This research also suggests that even in oligotrophic aquatic ecosystems, phytoplankton may bloom if the nutrient recycling rate after phytoplankton loss is high enough.

The light attenuation coefficient  $K_{bg}$  is an important index to evaluate the transmittance of water quality in an aquatic ecosystem. From Fig. 11, one can see that an increase of  $K_{bg}$  causes the spatial heterogeneity of phytoplankton in hypolimnion to change from aggregation to uniform distribution, and there is a shift of phytoplankton competition from hypolimnion to epilimnion. If the value of  $K_{bg}$  is low, which implies that the water has good light transmittance, phytoplankton in hypolimnion is a stronger competitor and inhibit the growth of phytoplankton in epilimnion. When the value of  $K_{bg}$  is high, the conclusion is just the opposite. Therefore, if the light transmittance of water is good, phytoplankton bloom will not likely occur, otherwise, it will.

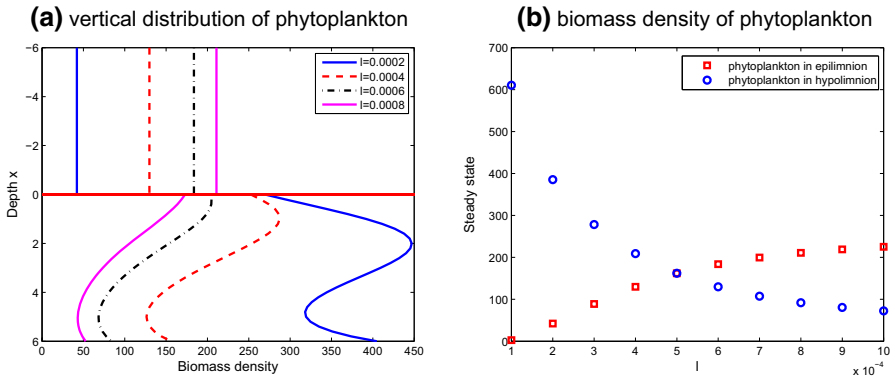


**Fig. 13** Influence of parameter  $l$  on the vertical distribution and biomass density of phytoplankton. The results show that high light attenuation coefficient  $l$  is more prone to phytoplankton blooms. Here other parameters are shown in Table 2

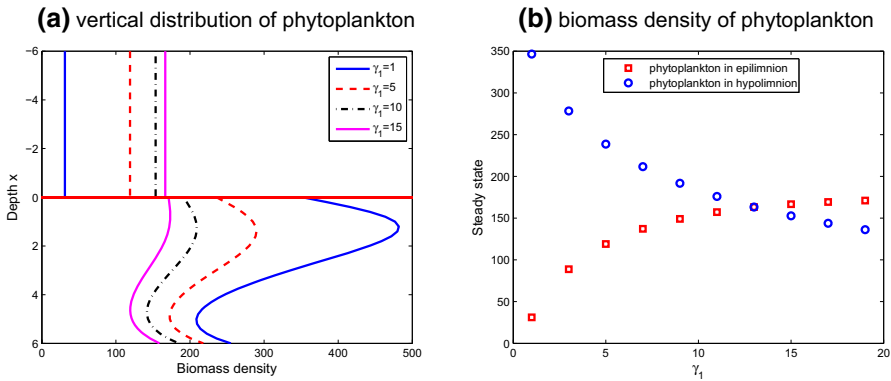


**Fig. 14** Influence of parameter  $\gamma_1$  on the vertical distribution and biomass density of phytoplankton. The results mean that with the increase in  $\gamma_1$ , the spatial heterogeneity of phytoplankton in the hypolimnion weakens and the possibility of blooms increases. Here other parameters are shown in Table 2

The nutrient to carbon quota  $\theta$  and light attenuation coefficient  $l$  describe the degree of phytoplankton growth requiring nutrients and light, respectively. Figure 12 shows that although the biomass density of phytoplankton in hypolimnion is almost unchanged with the increase in nutrient requirement, it gradually gathers from the top to bottom of hypolimnion. At the same time, the biomass density of phytoplankton in epilimnion decreases sharply. This implies that the requirement of phytoplankton for nutrients has a greater effect on phytoplankton in epilimnion, making it to change from a strong competitor to a weaker competitor. If phytoplankton need more light for the growth, then most of them gather in epilimnion, and their biomass density increases in the epilimnion and decreases in the hypolimnion (see Fig. 13). Therefore, phytoplankton with low nutrient requirement and high light requirement are more prone to bloom.

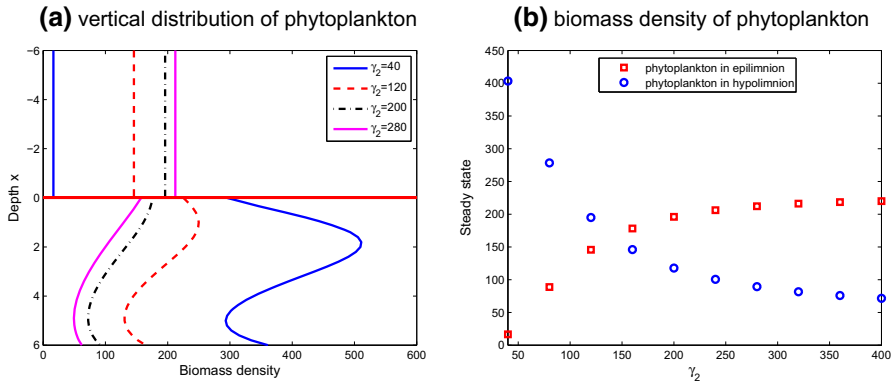


**Fig. 15** Influence of parameter  $\gamma_2$  on the vertical distribution and biomass density of phytoplankton. The results show that the increase of  $\gamma_2$  reduces the probability of phytoplankton blooms. Here other parameters are shown in Table 2

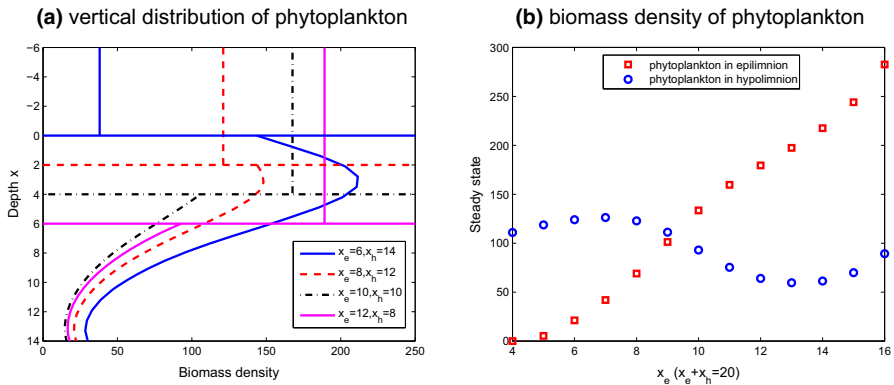


**Fig. 16** Influence of parameters  $x_e, x_h$  on the vertical distribution and biomass density of phytoplankton. The results show that the increase in  $x_e$  is easy to induce phytoplankton blooms, while the increase in  $x_h$  reduces the possibility of blooms. Here  $x_e + x_h = 20, D_m = D_b = 0.4$  and other parameters are shown in Table 2

The half saturation constants  $\gamma_1$  and  $\gamma_2$  characterize the efficiency of phytoplankton in absorbing nutrients and light, respectively. From Figs. 14 and 15, we observe that if the values of  $\gamma_1, \gamma_2$  are high, the spatial heterogeneity of phytoplankton in hypolimnion weakens and gradually turns into average distributed. In addition, phytoplankton in epilimnion become a stronger competitor, whose biomass density increases, and control the growth of phytoplankton in hypolimnion. There is a phytoplankton regime shift from hypolimnion to epilimnion. This means that if phytoplankton have high light or nutrient uptake efficiency, then the possibility of bloom will increase.

The depth of the thermocline between epilimnion and hypolimnion varies with the seasons, climate, latitude and local environmental conditions. When the thermocline descends, i.e., the value of  $x_e$  increases, the biomass density and aggregation layer of phytoplankton transfer from hypolimnion to epilimnion (see Fig. 16). On the contrary,

**Table 4** Influence of environmental parameters

Parameters	$x_{\max}$	BDPE	BDPH	PPB	Parameters	$x_{\max}$	BDPE	BDPH	PPB
$D_b, D_m \uparrow$	↓	↑	–	↑	$v \uparrow$	↑	↓↑	↑↓	–
$I_{in} \uparrow$	↑	↓	↑	↓	$M_b \uparrow$	↓	↑	–	↑
$p \uparrow$	↓	↑	–	↑	$K_{bg} \uparrow$	↓	↑	↓	↑
$\theta \uparrow$	↑	↓	–	↓	$l \uparrow$	↓	↑	↓	↑
$\gamma_1 \uparrow$	↓	↑	↓	↑	$\gamma_2 \uparrow$	↓	↑	↓	↑
$x_e \uparrow$	↓	↑	↑↓↑	↑	$x_h \uparrow$	↑	↓	↓↑↓	↓

↑: Increasing, ↓: Decreasing, –: No significant effect, *BDPE* Biomass density of phytoplankton in epilimnion, *BDPH* Biomass density of phytoplankton in hypolimnion, *PPB* Probability of phytoplankton blooms

if the thermocline ascends, then the biomass density and aggregation layer of phytoplankton transfer from epilimnion to hypolimnion. This also shows that phytoplankton blooms are easy to occur in summer or autumn. One of the reasons is that the increase in water temperature in these two seasons leads to the decline of the thermocline.

In order to summarize the above discussion, we let  $x_{\max}$  to be the depth coordinate, where the biomass density of phytoplankton in epilimnion and hypolimnion reaches its maximum.  $x_{\max}$  characterizes the change of phytoplankton aggregation layer. The increase means that the aggregation layer moves downward, while the decrease means that the aggregation layer moves upward. This indicates that  $x_{\max}$  is an index to describe the vertical distribution of phytoplankton. The influence of environmental parameters on the vertical distribution and biomass density of phytoplankton are listed in Table 4.

## 6 Discussion

We propose a mathematical model (2.1) to describe phytoplankton dynamics in a stratified lake. The existence and local stability of nonnegative steady-state solutions of model (2.1) are established in terms of parameters ( $\delta, a$ ) (the loss rate of phytoplankton and the settling speed of phytoplankton cells in the thermocline), and the results are summarized in Table 3.

Our analytical results on model (2.1) show that the extinction of phytoplankton in the epilimnion and hypolimnion may arise from the model for a larger phytoplankton loss rate. Phytoplankton in epilimnion and hypolimnion can coexist in a stratified lake if  $a = 0, p \in [0, 1)$  or  $0 < a < x_e \delta_0^*$  (see Figs. 2 and 3). In two extreme cases: (1) the settling speed rate is zero ( $a = 0$ ) and the nutrients are completely recycled ( $p = 1$ ); (2) the settling speed rate is large enough ( $a > x_e \delta_0^*$ ), the principle of competitive exclusion always holds. Model (2.1) including nonlocal effect and coupled dynamics of ODE and PDE equations is difficult for analyzing, and we obtain rigorous results for the existence and sometimes stability of nonnegative steady-state solutions in different parameter regions. It is important to understand the existence and stability of coexistence steady state  $E_4$  in parameter regions  $\Delta_{41}$  and  $\Delta_{43}$ , which is supported by our analytic results and extensive numerical simulations.

All the environmental parameters could influence the vertical distribution and biomass density of phytoplankton (see Table 4). Our studies demonstrate that high vertical turbulent diffusivity ( $D_b$ ,  $D_m$ ) in hypolimnion causes phytoplankton to accumulate in epilimnion and the increase of biomass density in epilimnion. This may result in the occurrence of phytoplankton blooms. Another spatial parameter  $v$  in hypolimnion has no obvious effect on phytoplankton blooms. High nutrient input concentration ( $M_b$ ), nutrient recycling proportion ( $p$ ), or nutrient uptake efficiency ( $\gamma_1$ ) reduces the dependence of phytoplankton in epilimnion on nutrients and makes it a stronger competitor. Hence, there is a biomass density regime shift from hypolimnion to epilimnion, which increases the probability of phytoplankton blooms. If phytoplankton are more dependent on light than nutrients, then high light attenuation coefficient ( $K_{bg}$ ), light requirement ( $l$ ) or light uptake efficiency ( $\gamma_2$ ) raises the possibility of phytoplankton blooms. Conversely, high light density ( $I_{in}$ ) or nutrient requirement ( $\theta$ ) reduces the possibility of phytoplankton blooms. The depths  $x_e$  and  $x_h$  of epilimnion and hypolimnion are also important environmental factors for the occurrence of phytoplankton blooms. The increase in epilimnion depth enhances the probability of phytoplankton blooms.

Lake stratification is a common phenomenon. The above theoretical analysis and numerical results characterize the vertical distribution and biomass change of phytoplankton in the epilimnion and hypolimnion. Phytoplankton in a stratified lake compete for light from the surface and nutrients from the benthic zone. This asymmetric resource supply mechanism is conducive to the coexistence of phytoplankton in the epilimnion and hypolimnion. The settling speed  $a$  is a key parameter for evaluating phytoplankton competition in a stratified lake. Both  $a = 0$  and  $a > x_e \delta_0^*$  can induce the principle of competitive exclusion. It is of great significance to measure the settling speed of phytoplankton cells in the thermocline for the assessment of phytoplankton dynamics in a stratified lake. Our studies show that the influence of water movement and depth, light, and nutrients on the vertical distribution and biomass change of phytoplankton and its internal mechanism (see Table 4 as a summary). These results can help control phytoplankton blooms and protect a freshwater ecosystem.

In Wang et al. (2007), Wang et al. investigated dynamics of stoichiometric bacterial-algae interactions in the epilimnion. This research was motivated by some hypotheses on competing bacterial strains observed in Lake Biwa (Nishimura et al. 2005). They pointed out that severely phosphorus limitation in the epilimnion is an important reason for low nucleic acid (LNA) bacteria to win the competition. However, they did not consider the interaction between algae and bacteria in the hypolimnion and its effect on the epilimnion. Compared with the literature (Wang et al. 2007), in the present paper, we consider phytoplankton dynamics in the epilimnion and hypolimnion and the interaction between them, and conclude that phytoplankton in the hypolimnion can control phytoplankton biomass in the epilimnion by controlling nutrient transport. Hence, an interesting but challenging question is to study the relationship between phytoplankton and bacteria in a stratified lake. Furthermore, it will be of interest to explore more biological questions including two or more species of phytoplankton (Du and Hsu 2010; Jiang et al. 2019; Mei and Zhang 2012), harmful phytoplankton (Hsu et al. 2013; Wang et al. 2015), as well as zooplankton and fishes (Hsu et al. 2013; Loladze et al. 2000; Lv et al. 2016).

## Appendix A

In order to obtain the existence and stability of semi-trivial steady-state solutions of (2.1), we consider an eigenvalue problem

$$\begin{cases} D\phi''(x) = \lambda\phi(x), & x \in (0, x_h), \\ D\phi'(0) = \frac{\lambda}{\delta_1\lambda + \delta_2}\phi(0), & \phi(x_h) = 0, \end{cases} \tag{A.1}$$

where  $D, \delta_1, \delta_2 > 0$ . A direct calculation shows that if  $\lambda$  is a complex eigenvalue of (A.1), then  $\bar{\lambda}$  is also a complex eigenvalue of (A.1).

**Lemma A.1** *If  $\lambda$  is an eigenvalue of (A.1), then  $\text{Re } \lambda < 0$ .*

**Proof** If  $\lambda$  is an eigenvalue (real or complex valued) and  $\phi(x)$  is the corresponding eigenfunction, then

$$\lambda \int_0^{x_h} |\phi(x)|^2 dx = D \int_0^{x_h} \phi''(x)\bar{\phi}(x) dx = -\frac{\lambda|\phi(0)|^2}{\delta_1\lambda + \delta_2} - D \int_0^{x_h} |\phi'(x)|^2 dx.$$

Let

$$c_1 = \int_0^{x_h} |\phi(x)|^2 dx, \quad c_2 = D \int_0^{x_h} |\phi'(x)|^2 dx.$$

Then,  $\lambda$  satisfies

$$\delta_1 c_1 \lambda^2 + (\delta_2 c_1 + |\phi(0)|^2 + \delta_1 c_2) \lambda + \delta_2 c_2 = 0.$$

This means that  $\text{Re } \lambda < 0$ . This completes the proof. □

**Proof of Theorem 3.1** From (3.1), it is easy to see that  $E_1 \equiv (0, M_b, 0, M_b)$  is the unique nutrients-only semi-trivial steady state solution of (2.1). The stability of  $E_1$  is determined by the eigenvalue problem

$$\lambda \xi = (\delta_a^* - \delta) \xi, \tag{A.2a}$$

$$\lambda \zeta = \theta \left( p\delta - \delta_a^* - \frac{a}{x_e} \right) \xi - \frac{b}{x_e} \zeta + \frac{b}{x_e} \psi(0), \tag{A.2b}$$

$$\lambda \varphi = D_b \varphi''(x) - v\varphi'(x) + (rf(M_b)g(I(x, 0, 0)) - \delta) \varphi, \quad 0 < x < x_h, \tag{A.2c}$$

$$\lambda \psi = D_m \psi''(x) + (\theta p\delta - \theta rf(M_b)g(I(x, 0, 0))) \varphi, \quad 0 < x < x_h, \tag{A.2d}$$

$$D_b \varphi'(0) - v\varphi(0) = -a\xi, \quad D_b \varphi'(x_h) - v\varphi(x_h) = 0, \tag{A.2e}$$

$$D_m \psi'(0) = b(\psi(0) - \zeta), \quad \psi(x_h) = 0. \tag{A.2f}$$

To establish the local stability of  $E_1$ , we let  $\lambda_1$  be the eigenvalue of (A.2) with the largest real part and let  $(\xi, \zeta, \varphi, \psi)$  be the corresponding eigenfunction. Note that the linearized system (A.2) is partially decoupled. We consider the following three cases: (i)  $\xi \neq 0$ ; (ii)  $\xi = 0, \varphi \neq 0$ ; or (iii)  $\xi = 0, \varphi \equiv 0$ .

Case (i):  $\xi \neq 0$ . In this case, the stability of  $E_1$  is determined by (A.2a). Then,  $\lambda_1 = \delta_a^* - \delta$ .

Case (ii):  $\xi = 0, \varphi \neq 0$ . This case means that the stability of  $E_1$  is determined by (A.2c) and its boundary condition (A.2e). Then,  $\lambda_1 = \delta_* - \delta$ .

Case (iii):  $\xi = 0, \varphi = 0$ . In this case, (A.2) reduces to

$$\begin{cases} \lambda \zeta = -\frac{b}{x_e} \zeta + \frac{b}{x_e} \psi(0), \\ \lambda \psi(x) = D_m \psi''(x), \quad 0 < x < x_h, \\ D_m \psi'(0) = b(\psi(0) - \zeta), \quad \psi(x_h) = 0. \end{cases} \tag{A.3}$$

From the boundary condition of (A.3), we have  $\zeta = 0$  if  $\psi \equiv 0$ . On the other hand, if  $\zeta = 0$  in (A.3), we also have  $\psi \equiv 0$ . This shows that  $\zeta \neq 0$  and  $\psi(x) \neq 0$ . Then, either  $\lambda = -b/x_e = -D_m k^2 \pi^2 / x_h^2$  for some  $k \in \mathbb{N}$  with the corresponding eigenfunction  $(\zeta, \psi) = (1, -\sqrt{bx_e/D_m} \sin(\sqrt{b/(x_e D_m)}x))$ ; or  $\lambda \neq -b/x_e, \zeta = \frac{b}{x_e \lambda + b} \psi(0)$ , and  $\psi$  satisfies

$$\begin{cases} \lambda \psi(x) = D_m \psi''(x), \quad 0 < x < x_h, \\ D_m \psi'(0) = \frac{bx_e \lambda}{x_e \lambda + b} \psi(0), \quad \psi(x_h) = 0. \end{cases} \tag{A.4}$$

It follows from Lemma A.1 that all eigenvalues of (A.4) have negative real parts. Therefore, we conclude that in case (iii),  $\text{Re } \lambda_1$  is negative.

Summarizing the above cases (i)-(iii), we conclude that if (3.6) holds, then  $\text{Re } \lambda_1 < 0$  and  $E_1$  is locally asymptotically stable; Conversely, if (3.7) holds, then  $\text{Re } \lambda_1 > 0$  and  $E_1$  is unstable.

Next we prove that if (3.8) holds, then  $E_1$  is globally asymptotically stable. From the first equation of (2.1), we have

$$\frac{dA(t)}{dt} \leq rA \frac{1}{x_e} \int_{-x_e}^0 g(I(x, 0))dx - \frac{a}{x_e} A - \delta A,$$

which implies that  $\lim_{t \rightarrow \infty} A(t) = 0$  if  $\delta > \delta_a^{**}$ . From the theory of asymptotical autonomous systems (Mischaikow et al. 1995), the third equation of (2.1) reduces to a limiting system

$$\begin{aligned} \frac{\partial B(x, t)}{\partial t} &= D_b \frac{\partial^2 B}{\partial x^2} - v \frac{\partial B}{\partial x} + rBf(M)g(I(x, A, B)) - \delta B \\ &\leq D_b \frac{\partial^2 B}{\partial x^2} - v \frac{\partial B}{\partial x} + rg(I(0, 0, 0))B - \delta B, \quad 0 < x < x_h, \quad t > 0, \\ D_b \frac{\partial B(0, t)}{\partial x} - vB(0, t) &= D_b \frac{\partial B(x_h, t)}{\partial x} - vB(x_h, t) = 0, \quad t > 0. \end{aligned}$$

This implies that  $B(x, t)$  converges to 0 uniformly for  $x \in [0, x_h]$  as  $t \rightarrow \infty$  if  $\delta > \delta_{**}$  by the comparison principle of parabolic equations. By applying the theory of asymptotical autonomous systems again, (2.1) reduces to a limiting system

$$\begin{cases} \frac{dN(t)}{dt} = \frac{b}{x_e}(M(0, t) - N(t)), & t > 0, \\ \frac{\partial M(x, t)}{\partial t} = D_m \frac{\partial^2 M}{\partial x^2}, & 0 < x < x_h, t > 0, \\ D_m \frac{\partial M(0, t)}{\partial x} = b(M(0, t) - N(t)), M(x_h, t) = M_b, & t > 0. \end{cases} \tag{A.5}$$

Define Lyapunov functional  $V : \mathbb{R} \times C([0, L]) \rightarrow \mathbb{R}$  by

$$V(N, M) = \frac{x_e}{2}(N - M_b)^2 + \frac{1}{2} \int_0^{x_h} (M(z) - M_b)^2 dz.$$

For an arbitrary solution  $(N(t), M(x, t))$  of (A.5) with nonnegative initial values, we obtain

$$\begin{aligned} \frac{dV(N(t), M(x, t))}{dt} &= x_e(N(t) - M_b) \frac{dN}{dt} + \int_0^{x_h} (M(z, t) - M_b) \frac{\partial M}{\partial t} dz \\ &= b(N(t) - M_b)(M(0, t) - N(t)) + D_m \int_0^{x_h} (M(z, t) - M_b) \frac{\partial^2 M}{\partial z^2} dz \\ &= b(N(t) - M_b)(M(0, t) - N(t)) \\ &\quad + D_m \frac{\partial M}{\partial z} (M(z, t) - M_b) \Big|_0^{x_h} - \int_0^{x_h} \left( \frac{\partial M}{\partial z} \right)^2 dz \\ &= b(N(t) - M_b)(M(0, t) - N(t)) \\ &\quad - b(M(0, t) - N(t))(M(0, t) - M_b) - \int_0^{x_h} \left( \frac{\partial M}{\partial z} \right)^2 dz \\ &= -b(N(t) - M(0, t))^2 - \int_0^{x_h} \left( \frac{\partial M}{\partial z} \right)^2 dz \leq 0. \end{aligned}$$

Note that  $dV(\cdot)/dt = 0$  holds if and only if  $\partial M/\partial z = 0$  and  $N(t) = M(0, t)$ . It follows from  $M(x_h, t) = M_b$  that  $N(t) \equiv M(x, t) \equiv M_b$ . By using the LaSalle’s Invariance Principle (Henry 1981), we conclude that  $(N(t), M(x, t))$  converges to  $(M_b, M_b)$  uniformly for  $x \in [0, x_h]$  as  $t \rightarrow \infty$ , and  $E_1$  is globally asymptotically stable for (2.1) with respect to any nonnegative initial value.  $\square$

**Proof of Theorem 3.3** The steady-state equation (3.2) can be explicitly solved. The equation of  $N$  implies that  $b(M(0) - N) = (1 - p)\theta\delta x_e A$ . Combining the equation of  $M$  with its boundary conditions  $D_m M'(0) = (1 - p)\theta\delta x_e A$  and  $M(x_h) = M_b$  gives

$$M(x) = M_b - \frac{x_h - x}{D_m} (1 - p)\theta\delta x_e A,$$

and then

$$N = M_b - \left( \frac{x_h}{D_m} + \frac{1}{b} \right) (1 - p)\theta\delta x_e A.$$

If  $p = 1$  and (3.9) holds, then  $M(x) = N = M_b$ , and there exists a unique positive  $A_2^*$  satisfying  $f(M_b) \frac{r}{x_e} \int_{-x_e}^0 g(I(x, A_2^*)) dx = \delta$  since  $g$  is a strictly decreasing function of  $A$ . If  $p \in [0, 1)$ , then we let

$$Q = \delta A, \quad \beta = \left( \frac{x_h}{D_m} + \frac{1}{b} \right) (1 - p)\theta x_e.$$

From the first equation of (3.2), we consider

$$u(\delta, Q) = \frac{r}{x_e} \int_{-x_e}^0 g\left(I\left(x, \frac{Q}{\delta}\right)\right) dx - \delta \left(1 + \frac{\gamma_1}{M_b - \beta Q}\right) \text{ for } (\delta, Q) \in (0, \infty) \\ \times \left(0, \frac{M_b}{\beta}\right).$$

A direct calculation gives  $\partial u / \partial Q < 0$ . Note that  $\lim_{Q \rightarrow 0^+} u(\delta, Q) = (1 + \gamma_1 / M_b)(\delta_0^* - \delta) > 0$  if  $0 < \delta < \delta_0^*$  and  $\lim_{Q \rightarrow (M_b/\beta)^-} u(\delta, Q) = -\infty$ . Then for any fixed  $\delta \in (0, \delta_0^*)$ , there exists a unique positive  $Q_\delta$  such that  $u(\delta, Q_\delta) = 0$ , and  $A_2^* = Q_\delta / \delta$  is desired unique solution. This proves part (i).

Next we establish the stability of  $E_2$ . The stability of  $E_2$  is determined by the eigenvalue problem

$$\lambda \xi = -h_1 \xi + h_2 \zeta, \tag{A.6a}$$

$$\lambda \zeta = -(1 - p)\theta\delta + \theta h_1) \xi - \left( \frac{b}{x_e} + \theta h_2 \right) \zeta + \frac{b}{x_e} \psi(0), \tag{A.6b}$$

$$\lambda \varphi = D_b \varphi''(x) - v \varphi'(x) + (h_3(x) - \delta) \varphi, \quad 0 < x < x_h, \tag{A.6c}$$

$$\lambda \psi = D_m \psi''(x) + (p\theta\delta - \theta h_3(x)) \varphi, \quad 0 < x < x_h, \tag{A.6d}$$

$$D_b \varphi'(0) - v \varphi(0) = D_b \varphi'(x_h) - v \varphi(x_h) = 0, \tag{A.6e}$$

$$D_m \psi'(0) = b(\psi(0) - \zeta), \quad \psi(x_h) = 0, \tag{A.6f}$$

where

$$h_1 = \frac{r\gamma_2 \mu(A_2^*) N_2^* A_2^*}{N_2^* + \gamma_1}, \quad h_2 = \frac{r\gamma_1 A_2^*}{(N_2^* + \gamma_1)^2} \frac{1}{x_e} \int_{-x_e}^0 g(I(x, A_2^*)) dx, \tag{A.7} \\ h_3(x) = r f(M_2^*) g(I(x, A_2^*), 0))$$

and

$$\mu(A_2^*) = \frac{l \left( \ln \frac{I_{in} + \gamma_2}{I_{in}e^{-x_e(K_{bg} + lA_2^*)} + \gamma_2} - \frac{I_{in}x_e(K_{bg} + lA_2^*)e^{-x_e(K_{bg} + lA_2^*)}}{I_{in}e^{-x_e(K_{bg} + lA_2^*)} + \gamma_2} \right)}{x_e(K_{bg} + lA_2^*)^2} > 0. \tag{A.8}$$

Again let  $\lambda_1$  be the eigenvalue of (A.6) with largest real part, and let  $(\xi, \zeta, \varphi, \psi)$  be the corresponding eigenfunction. Note that the eigenvalue problem (A.6) is partially decoupled. We consider the following two cases: (i)  $\varphi \neq 0$ ; (ii)  $\varphi \equiv 0$ .

Case (i):  $\varphi \neq 0$ . Then, the stability of  $E_2$  is determined by the subsystem

$$\begin{aligned} \lambda\varphi &= D_b\varphi''(x) - v\varphi'(x) + (h_3(x) - \delta)\varphi, \quad 0 < x < x_h, \\ D_b\varphi'(0) - v\varphi(0) &= D_b\varphi'(x_h) - v\varphi(x_h) = 0, \end{aligned} \tag{A.9}$$

with  $\xi, \zeta, \psi$  solved from (A.6a), (A.6b), (A.6d) and (A.6f). Then,  $\lambda_1 = \lambda_1(D_b, v, h_3(x) - \delta) = \lambda_1(D_b, v, h_3(x)) - \delta$ .

Case (ii):  $\varphi \equiv 0$ . Then,  $(\xi, \zeta, \psi)$  satisfies

$$\begin{aligned} \lambda\xi &= -h_1\xi + h_2\zeta, \\ \lambda\zeta &= -(1 - p)\theta\delta + \theta h_1)\xi - \left( \frac{b}{x_e} + \theta h_2 \right) \zeta + \frac{b}{x_e} \psi(0), \\ \lambda\psi &= D_m\psi''(x), \quad 0 < x < x_h, \\ D_m\psi'(0) &= b(\psi(0) - \zeta), \quad \psi(x_h) = 0. \end{aligned} \tag{A.10}$$

By using similar arguments as those in Theorem 3.1 and Lemma A.1, we conclude that all eigenvalues of (A.10) have negative real parts. Based on the analysis above,  $E_2$  is locally asymptotically stable with respect to (2.1) if (3.11) holds, while  $E_2$  is unstable if (3.12) holds.

It can be shown that  $A_2^*$  is strictly decreasing in  $\delta$  and  $\lim_{\delta \rightarrow \delta_0^{*-}} A_2^* = 0$ . This also implies that  $\lim_{\delta \rightarrow \delta_0^{*-}} N_2^* = M_b$  and  $\lim_{\delta \rightarrow \delta_0^{*-}} M_2^*(x) = M_b$ . Hence, when  $\delta \rightarrow \delta_0^{*-}$ , we have

$$\begin{aligned} &\lim_{\delta \rightarrow \delta_0^{*-}} \left[ \lambda_1(D_b, v, rf(M_2^*)g(I(x, A_2^*), 0)) - \delta \right] \\ &= \lim_{\delta \rightarrow \delta_0^{*-}} \left[ \lambda_1(D_b, v, rf(M_2^*)g(I(x, A_2^*), 0)) \right. \\ &\quad \left. - \lambda_1 \left( D_b, v, f(N_2^*) \frac{r}{x_e} \int_{-x_e}^0 g(I(x, A_2^*)) dx \right) \right] \\ &= \lambda_1(D_b, v, rf(M_b)g(I(x, 0, 0))) - \lambda_1 \left( D_b, v, f(M_b) \frac{r}{x_e} \int_{-x_e}^0 g(I(x, 0)) dx \right) < 0. \end{aligned}$$

Therefore, (3.11) holds and  $E_2$  is locally asymptotically stable when  $\delta$  is sufficiently close to  $\delta_0^*$ . When  $p = 1$ ,  $E_2 \equiv (A_2^*, M_b, 0, M_b)$  where  $A_2^*$  satisfies (3.10) with  $N_2^* = M_b$ . From (3.5) and the monotonicity of the principal eigenvalue on the weight functions, we have

$$\lambda_1(D_b, v, rf(M_b)g(I(x, A_2^*, 0))) < \lambda_1\left(D_b, v, f(M_b)\frac{r}{x_e} \int_{-x_e}^0 g(I(x, A_2^*))dx\right) = \delta,$$

so (3.11) holds and  $E_2$  is locally asymptotically stable for any  $0 < \delta < \delta_0^*$ . □

To obtain the global existence of  $E_3$ , we first establish the following *a priori* estimates for nonnegative solutions  $(N_3, B_3(x), M_3(x))$  of (3.3).

**Lemma A.2** *Assume that  $(N_3, B_3(x), M_3(x)) \in \mathbb{R}^+ \times Y^2$  is a nonnegative solution of (3.3) with  $N_3 > 0, B_3, M_3 \not\equiv 0$ . Then,*

- (i)  $0 < \delta < \delta_{**}$ , where  $\delta_{**}$  is defined in (3.5);
- (ii) For any  $\epsilon > 0$ , there exists a positive constant  $K(\epsilon)$  such that  $0 < B_3(x) \leq K(\epsilon)$  and  $0 < N_3, M_3(x) \leq M_b + \theta x_h^2(r + p\delta_{**})K(\epsilon)/D_m$  on  $[0, x_h]$  for  $\delta \in [\epsilon, \delta_{**}]$ .

**Proof** (i) Let  $R(x) = B_3(x)e^{-(v/D_b)x}$ . Then,  $R(x)$  satisfies

$$\begin{cases} -D_b R''(x) - vR'(x) + \delta R = rf(M_3)g(I(x, 0, B_3))R \geq 0, & 0 < x < x_h, \\ R'(0) = 0, R'(x_h) = 0. \end{cases}$$

It follows from the strong maximum principle that  $R(x) > 0$  on  $[0, x_h]$ , and consequently,  $B_3(x) > 0$  on  $[0, x_h]$ . From (3.3), we have

$$\lambda_1(D_b, v, rf(M_3)g(I(x, 0, B_3))) = \delta$$

with corresponding principal eigenfunction  $B_3$ . It follows from the monotonicity of principal eigenvalue with respect to the weight functions that

$$\delta = \lambda_1(D_b, v, rf(M_3)g(I(x, 0, B_3))) < \lambda_1(D_b, v, rg(I(0, 0, 0))) = \delta_{**}.$$

(ii) Fix  $\epsilon > 0$ . If  $B_3$  is not bounded for all  $\delta \in [\epsilon, \delta_{**}]$ , then there are a sequence  $\delta^i \in [\epsilon, \delta_{**}]$  and corresponding positive solutions  $(N_3^i, B_3^i(x), M_3^i(x))$  such that  $\|B_3^i\|_\infty \rightarrow \infty$  and  $\delta^i \rightarrow \delta^0 \in [\epsilon, \delta_{**}]$  as  $i \rightarrow \infty$ . Let  $\mu_i = B_3^i/\|B_3^i\|_\infty$ . From the equation of  $B_3$  in (3.3), we get

$$\begin{cases} -D_b \mu_i''(x) + v\mu_i'(x) = [rf(M_3^i)g(I(x, 0, B_3^i)) - \delta^i]\mu_i(x) = 0, & 0 < x < x_h, \\ D_b \mu_i'(0) - v\mu_i(0) = D_b \mu_i'(x_h) - v\mu_i(x_h) = 0. \end{cases} \tag{A.11}$$

Since the right hand side of (A.11) is uniformly bounded, by using  $L^p$  theory for elliptic operators and by passing to a subsequence, we obtain that  $\mu_i \rightarrow \mu$

in  $W^{2,p}([0, x_h])$  (and also in  $C^{1,\alpha}([0, x_h])$  from Sobolev’s embedding) as  $i \rightarrow \infty$ . Since  $rf(M_3^i)g(I(x, 0, B_3^i))$  is bounded in  $L^\infty([0, x_h])$ , we may assume that  $rf(M_3^i)g(I(x, 0, B_3^i)) \rightarrow l^0$  weakly in  $L^2([0, x_h])$ . Hence,  $\mu$  satisfies (in the weak sense)

$$\begin{cases} D_b\mu''(x) - v\mu'(x) + (l^0 - \delta^0)\mu(x) = 0, & 0 < x < x_h, \\ D_b\mu'(0) - v\mu(0) = D_b\mu'(x_h) - v\mu(x_h) = 0. \end{cases} \tag{A.12}$$

From the strong maximum principle,  $\mu(x) > 0$  on  $[0, x_h]$  since  $\mu \geq 0$  and  $\|\mu\|_\infty = 1$ . This implies that  $B_3^i = \|B_3^i\|_\infty \mu_i \rightarrow \infty$  uniformly on  $[0, x_h]$ , and thus,  $l^0 = 0$ . Integrating (A.12) we obtain  $0 = \delta^0 \int_0^{x_h} \mu(x)dx > 0$ . That is a contradiction. Therefore, there is a positive constant  $K(\epsilon)$  such that  $0 < B_3(x) \leq K(\epsilon)$  on  $[0, x_h]$  for all  $\delta \in [\epsilon, \delta_{**})$ .

From the strong maximum principle, we have  $M_3(x) > 0$  on  $[0, x_h]$ . For any  $x \in [0, x_h]$ , we have

$$\begin{aligned} |D_m M_3'(x)| &= \left| D_m \int_0^x M_3'(s)ds \right| = \theta \left| \int_0^x (rf(M_3)g(I(x, 0, B_3)) - p\delta) B_3 ds \right| \\ &\leq \theta x_h (r + p\delta_{**}) K(\epsilon) \end{aligned}$$

and consequently

$$\begin{aligned} |M_3(x)| &= |M_3(x_h) + M_3(x) - M_3(x_h)| \leq |M_3(x_h)| + |M_3(x) - M_3(x_h)| \\ &\leq M_b + \left| \int_x^{x_h} M_3'(s)ds \right| \leq M_b + \theta x_h^2 (r + p\delta_{**}) K(\epsilon) / D_m. \end{aligned} \tag{A.13}$$

From  $M_3(0) = N_3$ , we have  $0 < N_3 \leq M_b + \theta x_h^2 (r + p\delta_{**}) K(\epsilon) / D_m$ . □

**Proof of Theorem 3.5** We prove the existence of  $E_3$  using bifurcation theory and show that the solution  $E_3$  bifurcates from the line of nutrient-only semi-trivial steady state  $E_1$  at  $\delta = \delta_*$  with parameter  $\delta$ . We first use local bifurcation theory in Crandall and Rabinowitz (1971) to show that  $E_3$  bifurcates from the line of  $E_1$  at  $\delta = \delta_*$ .

Recall function spaces  $X_1, X_2$  defined in (3.13) and define  $Y = C([0, x_h])$ . We define a nonlinear mapping  $F : \mathbb{R}^+ \times \mathbb{R} \times X_1 \times X_2 \rightarrow \mathbb{R} \times Y^2 \times \mathbb{R}^2$  by

$$F(\delta, N, B, M) = \begin{pmatrix} M(0) - N \\ D_b B'' - vB' + rBf(M)g(I(x, 0, B)) - \delta B \\ D_m M'' + \theta p\delta B - \theta rBf(M)g(I(x, 0, B)) \\ D_m M'(0) - b(M(0) - N) \\ M(x_h) - M_b \end{pmatrix}.$$

It is easy to see that  $F(\delta, M_b, 0, M_b) = 0$ . Let  $H := F_{(N, B, M)}(\delta_*, M_b, 0, M_b)$  be the Frechét derivative of  $F$  with respect to  $(N, B, M)$  at  $(\delta_*, M_b, 0, M_b)$ . For any

$(\zeta, \varphi, \psi) \in \mathbb{R} \times X_1 \times X_2$ , we have

$$H[\zeta, \varphi, \psi] = \begin{pmatrix} \psi(0) - \zeta \\ D_b \varphi''(x) - v\varphi'(x) + (rf(M_b)g(I(x, 0, 0)) - \delta_*) \varphi \\ D_m \psi''(x) + (\theta p\delta_* - \theta rf(M_b)g(I(x, 0, 0))) \varphi \\ D_m \psi'(0) - b(\psi(0) - \zeta) \\ \psi(x_h) \end{pmatrix}. \tag{A.14}$$

If  $(\zeta_1, \varphi_1, \psi_1) \in \ker H$ , then

$$\psi_1(0) - \zeta_1 = 0, \tag{A.15a}$$

$$D_b \varphi_1''(x) - v\varphi_1'(x) + (rf(M_b)g(I(x, 0, 0)) - \delta_*) \varphi_1 = 0, \quad 0 < x < x_h, \tag{A.15b}$$

$$D_m \psi_1''(x) + (\theta p\delta_* - \theta rf(M_b)g(I(x, 0, 0))) \varphi_1 = 0, \quad 0 < x < x_h, \tag{A.15c}$$

$$\psi_1'(0) = 0, \quad \psi_1(x_h) = 0. \tag{A.15d}$$

Recall that  $\delta_*$  is the principal eigenvalue of (3.4) with  $q(x) = rf(M_b)g(I(x, 0, 0))$ , and let  $\bar{\varphi} \in X_1$  be the corresponding positive eigenfunction for the principal eigenvalue  $\delta_*$ . Then,  $\bar{\varphi}$  is the unique solution of (A.15b) up to a constant multiple. And there exist unique functions  $\bar{\psi} \in X_2$  and  $\bar{\zeta} \in \mathbb{R}$  satisfying (A.15c), (A.15d) and (A.15a). Hence,  $\dim \ker H = 1$  and  $\ker H = \text{span}\{\bar{\zeta}, \bar{\varphi}, \bar{\psi}\}$ .

If  $(\sigma_1, \sigma_2, \sigma_3, \sigma_4, \sigma_5) \in \text{range } H$ , then there exists  $(\zeta_2, \varphi_2, \psi_2) \in \mathbb{R} \times X_1 \times X_2$  such that

$$\psi_2(0) - \zeta_2 = \sigma_1,$$

$$D_b \varphi_2''(x) - v\varphi_2'(x) + (rf(M_b)g(I(x, 0, 0)) - \delta_*) \varphi_2 = \sigma_2(x), \quad 0 < x < x_h, \tag{A.16}$$

$$D_m \psi_2''(x) + (\theta p\delta_* - \theta rf(M_b)g(I(x, 0, 0))) \varphi_2 = \sigma_3(x), \quad 0 < x < x_h,$$

$$D_m \psi_2'(0) - b(\psi_2(0) - \zeta_2) = \sigma_4, \quad \psi_2(x_h) = \sigma_5.$$

Multiplying both sides of (A.15b) and the second equation of (A.16) by  $\varphi_2 e^{-(v/D_b)x}$  and  $\varphi_1 e^{-(v/D_b)x}$ , respectively, subtracting, and integrating on  $[0, x_h]$ , we obtain

$$\begin{aligned} & \int_0^{x_h} \sigma_2(x) e^{-(v/D_b)x} \varphi_1(x) dx \\ &= D_b \int_0^{x_h} \left( \left( \varphi_2'(x) e^{-(v/D_b)x} \right)' \varphi_1(x) - \left( \varphi_1'(x) e^{-(v/D_b)x} \right)' \varphi_2(x) \right) dx \\ &= D_b \varphi_2'(x) e^{-(v/D_b)x} \varphi_1(x) \Big|_0^{x_h} - D_b \varphi_1'(x) e^{-(v/D_b)x} \varphi_2(x) \Big|_0^{x_h} = 0. \end{aligned}$$

This implies that

$$\int_0^{x_h} \sigma_2(x) e^{-(v/D_b)x} \bar{\varphi}(x) dx = 0$$

and

$$\text{range } H = \left\{ (\sigma_1, \sigma_2, \sigma_3, \sigma_4, \sigma_5) \in \mathbb{R} \times Y^2 \times \mathbb{R}^2 : \int_0^{x_h} \sigma_2(x) e^{-(v/D_b)x} \bar{\varphi}(x) dx = 0 \right\}.$$

Then,  $\text{codim range } H = 1$ . Moreover, we also have

$$F_{\delta(N,B,M)}(\delta_*, M_b, 0, M_b)(\bar{\zeta}, \bar{\varphi}, \bar{\psi}) = (0, -\bar{\varphi}, p\theta\bar{\varphi}, 0, 0),$$

so  $F_{\delta(N,B,M)}(\delta_*, M_b, 0, M_b)(\bar{\zeta}, \bar{\varphi}, \bar{\psi}) \notin \text{range } H$  as  $\int_0^{x_h} \sigma_2(x) e^{-(v/D_b)x} \bar{\varphi}^2(x) dx \neq 0$ .

From Theorem 1.7 in Crandall and Rabinowitz (1971), there exists a positive constant  $\varepsilon_3 > 0$  such that all solutions of (3.3) near  $(\delta_*, M_b, 0, M_b)$  lie on a smooth curve

$$\Gamma_3 = \{(\delta_3(s), N_3^*(s), B_3^*(s, x), M_3^*(s, x)) : 0 < s < \varepsilon_3\}$$

with the form

$$\begin{cases} N_3^*(s) = M_b + s\bar{\zeta} + o(s), & B_3^*(s, x) = s\bar{\varphi}(x) + o(s), \\ M_3^*(s, x) = M_b + s\bar{\psi}(x) + o(s). \end{cases} \tag{A.17}$$

Let  $\bar{l}$  be a linear functional on  $\mathbb{R} \times Y^2 \times \mathbb{R}^2$  by

$$\langle \bar{l}, (\sigma_1, \sigma_2, \sigma_3, \sigma_4, \sigma_5) \rangle = \int_0^{x_h} \sigma_2(x) e^{-(v/D_b)x} \bar{\varphi}(x) dx.$$

Then, from Liu et al. (2007), we have

$$\begin{aligned} \delta_3'(0) &= -\frac{\langle \bar{l}, F_{(N,B,M)(N,B,M)}(\delta_*, M_b, 0, M_b) [\bar{\zeta}, \bar{\varphi}, \bar{\psi}]^2 \rangle}{2 \langle \bar{l}, F_{\delta(N,B,M)}(\delta_*, M_b, 0, M_b) [\bar{\zeta}, \bar{\varphi}, \bar{\psi}] \rangle} \\ &= -\frac{\int_0^{x_h} \frac{r I(x, 0, 0) e^{-(v/D_b)x}}{(M_b + \gamma_1)(I(x, 0, 0) + \gamma_2)} \mu(x, \bar{\varphi}, \bar{\psi}) dx}{\int_0^{x_h} e^{-(v/D_b)x} \bar{\varphi}^2(x) dx}, \end{aligned} \tag{A.18}$$

where

$$\mu(x, \bar{\varphi}, \bar{\psi}) = \frac{\gamma_2 I M_b}{I(x, 0, 0) + \gamma_2} \bar{\varphi}^2(x) \int_0^x \bar{\varphi}(s) ds - \frac{\gamma_1}{M_b + \gamma_1} \bar{\varphi}^2(x) \bar{\psi}(x), \quad x \in [0, x_h].$$

We claim that  $\bar{\psi}(x) \leq 0$  on  $x \in [0, x_h]$ . Let  $y(x) = rf(M_b)g(I(x, 0, 0))$ . Then  $y(x)$  is a strictly decreasing function on  $x \in [0, x_h]$ . It follows from (A.15b)-(A.15d) that  $\bar{\psi}'(x_h) \geq 0$ . From (A.15c), we have  $\bar{\psi}''(x) > 0$  on  $x \in [0, x_h]$  if  $p \leq y(x_h)/\delta_*$ .

Combining with its boundary conditions  $\bar{\psi}'(x) = 0, \bar{\psi}(x_h) = 0$ , we get  $\bar{\psi}(x) \leq 0$  on  $x \in [0, x_h]$ . If  $p > y(x_h)/\delta_*$ , then there is a unique  $x_0 \in (0, x_h)$  such that  $\bar{\psi}''(x) > 0$  on  $x \in (0, x_0)$  and  $\bar{\psi}''(x) < 0$  on  $x \in (x_0, x_h)$ . This means that  $\bar{\psi}'(x)$  is a strictly increasing function on  $x \in [0, x_0)$  and a strictly decreasing function on  $x \in (x_0, x_h]$ . Hence  $\bar{\psi}'(x) > 0$  on  $x \in (0, x_h)$  since  $\bar{\psi}'(0) = 0$  and  $\bar{\psi}'(x_h) \geq 0$ . It follows from  $\bar{\psi}(x_h) = 0$  that  $\bar{\psi}(x) \leq 0$  on  $x \in [0, x_h]$ . From (A.18), we have  $\delta_3'(0) < 0$ , which implies that the bifurcation at  $(\delta_*, M_b, 0, M_b)$  is backward. This completes the proof of part (iii).

Now we turn to global bifurcation of solutions of (3.3). By using Theorem 3.3 and Remark 3.4 in Shi and Wang (2009), we conclude that there exists a connected component  $\Lambda^+$  of  $\Lambda$  containing  $\Gamma_3$ , and the closure of  $\Lambda^+$  includes the bifurcation point  $(\delta_*, M_b, 0, M_b)$ . Moreover,  $\Lambda^+$  satisfies one of the following three alternatives:

- (a) it is not compact in  $\mathbb{R}^+ \times \mathbb{R} \times X_1 \times X_2$ ;
- (b) it contains another bifurcation point  $(\hat{\delta}, M_b, 0, M_b)$  with  $\hat{\delta} \neq \delta_*$ ;
- (c) it contains a point  $(\delta, M_b + N_3^{**}, B_3^{**}(x), M_b + M_3^{**}(x))$  with  $0 \neq (N_3^{**}, B_3^{**}(x), M_3^{**}(x)) \in \mathcal{W}$ , where  $\mathcal{W}$  is a closed complement of  $\ker H = \text{span}(\zeta, \bar{\varphi}, \bar{\psi})$  in  $\mathbb{R} \times X_1 \times X_2$ .

If the alternative (c) holds, then

$$\int_0^{x_h} B_3^{**}(x)\bar{\varphi}(x)dx = 0. \tag{A.19}$$

But it follows from Lemma A.2 that  $B_3^{**}(x) > 0$  on  $[0, x_h]$ , and  $\bar{\varphi}(x) > 0$  as it is a positive eigenfunction. This is a contradiction to (A.19), which means that (c) cannot happen. Suppose that the alternative (b) occurs, then (A.15) has a nonzero solution  $(\hat{\zeta}, \hat{\varphi}, \hat{\psi})$  with  $\delta_*$  replaced by  $\hat{\delta}, \hat{\varphi} \in X_1$ , and  $\hat{\varphi} > 0$ . But the eigenvalue problem (3.4) has only one eigenvalue with positive eigenfunction, hence (b) cannot happen either.

Therefore, the alternative (a) must happen, and  $\Lambda^+$  is not compact in  $\mathbb{R}^+ \times \mathbb{R} \times X_1 \times X_2$ . From Lemma A.2,  $(N_3^*, B_3^*(x), M_3^*(x))$  is bounded on  $[0, x_h]$  for  $\delta \in [\epsilon, \delta_{**})$  with any  $\epsilon > 0$ , and (3.3) has no nonnegative solution when  $\delta > \delta_{**}$ . Hence the projection of  $\Lambda^+$  onto  $\delta$ -axis is contained in  $(0, \delta_{**})$ , but contains  $[\epsilon, \delta_*)$  for any  $\epsilon > 0$ , so the projection of  $\Lambda^+$  onto  $\delta$ -axis contains  $(0, \delta_*)$ . This also implies that there is at least one positive solution of (3.3) on  $\Lambda^+$  for any  $\delta \in (0, \delta_*)$ . This completes the proof of parts (i) and (ii). □

To prove the existence of coexistence steady state  $E_4$ , we first prove the following elementary result.

**Lemma A.3** *Suppose that  $0 < a < x_e(\delta_0^* - \delta_*)$  holds, then*

$$\begin{cases} D_b\varphi''(x) - v\varphi'(x) + (rf(M_b)g(I(x, 0, 0)) - \delta_a^*)\varphi = 0, & 0 < x < x_h, \\ D_b\varphi'(0) - v\varphi(0) = -a, \quad D_b\varphi'(x_h) - v\varphi(x_h) = 0. \end{cases} \tag{A.20}$$

has a unique positive solution  $\hat{\varphi}(x)$ .

**Proof** By using the transform  $\phi(x) = \varphi(x)e^{-(v/D_b)x}$ , we get

$$\begin{cases} D_b\phi''(x) + v\phi'(x) + (rf(M_b)g(I(x, 0, 0)) - \delta_a^*)\phi = 0, & 0 < x < x_h, \\ -D_b\phi'(0) - a = 0, \phi'(x_h) = 0. \end{cases} \tag{A.21}$$

It is clear that 0 is a lower solution of (A.21). Let  $\tilde{\varphi}(x) = \tilde{\phi}(x)e^{(v/D_b)x}$  be the positive eigenfunction of (3.4) corresponding to  $\lambda_1(D_b, v, rf(M_b)g(I(x, 0, 0)) = \delta_*$  with  $\max_{x \in [0, x_h]} \tilde{\phi}(x) = 1$ . Define  $\bar{\phi}(x) = K[\tilde{\phi}(x) + \epsilon(x - x_h)^2]$ , where  $K$  and  $\epsilon$  are positive constants to be specified. Then

$$\begin{aligned} & D_b\bar{\phi}''(x) + v\bar{\phi}'(x) + (rf(M_b)g(I(x, 0, 0)) - \delta_a^*)\bar{\phi} \\ &= (\delta_* - \delta_a^*)K\tilde{\phi} + \epsilon K \left[ 2D_b + 2v(x - x_h) + (rf(M_b)g(I(x, 0, 0)) - \delta_a^*)(x - x_h)^2 \right] \\ &\leq 0, \quad 0 < x < x_h, \end{aligned}$$

if  $\epsilon > 0$  is chosen sufficiently small since  $\delta_* - \delta_a^* < 0$  and  $\tilde{\phi} > 0$ . We can further choose  $K > 0$  so that  $-D_b\bar{\phi}'(0) - a = 2D_bK\epsilon x_h - a = 0$  and  $\bar{\phi}'(x_h) = 0$ .

Hence  $\bar{\phi}$  is an upper solution of (A.21). From Theorem 3.2.1 in Pao (1992), there is a solution  $\hat{\phi}$  of (A.21) satisfying  $0 \leq \hat{\phi} \leq \bar{\phi}$ . It follows from the strong maximum principle that  $\hat{\phi} > 0$ . Note that (A.21) is a linear ODE with nonhomogeneous boundary conditions. Hence  $\hat{\phi}$  is unique. This implies that there exists a unique positive solution  $\hat{\phi} = \hat{\phi}e^{(v/D_b)x}$  of (A.20). □

To obtain the global existence of  $E_4$ , we first establish the following *a priori* estimates for nonnegative solutions  $(A_4, N_4, B_4(x), M_4(x))$  of (3.14).

**Lemma A.4** Assume that  $(A_4, N_4, B_4, M_4) \in (\mathbb{R}^+)^2 \times Y^2$  is a nonnegative solution of (3.14) with  $A_4, N_4 > 0$  and  $B_4, M_4 \not\equiv 0$ . Then

- (i)  $0 < \delta < \delta_a^{**}$ , where  $\delta_a^{**}$  is defined in (3.5);
- (ii)  $0 < A_4 < K$ , where  $K$  satisfies  $\frac{r}{x_e} \int_{-x_e}^0 g(I(x, K))dx = \delta + \frac{a}{x_e}$ ;
- (iii) For any  $\epsilon > 0$ , there exists a positive constant  $C(\epsilon) > 0$  such that

$$\begin{aligned} 0 < B_4(x) &\leq C(\epsilon), \\ 0 < N_4, M_4(x) &< M_b + x_h^2\theta(r + p\delta_a^{**})C(\epsilon)/D_m + x_h\theta(x_e(1 - p)\delta_a^{**} + a)K/D_m \end{aligned}$$

on  $[0, x_h]$  for  $\delta \in [\epsilon, \delta_a^{**})$ .

**Proof** It follows from the first equation of (3.14) that (i) and (ii) hold. By applying similar arguments to those in Lemma A.2, we conclude that  $M_4 > 0$  and for any  $\epsilon > 0$ , there exists a positive constant  $C(\epsilon) > 0$  such that  $0 < B_4 \leq C(\epsilon)$ . From the second and fourth equations of (3.14), we have

$$b(M_4(0) - N_4) = \theta(x_e(1 - p)\delta + a)A_4$$

and

$$\begin{aligned}
 |D_m M'_4(x)| &= \left| D_m \int_0^x M''_4(s) ds + D_m M'_4(0) \right| \\
 &\leq \theta \left| \int_0^x (rf(M_4)g(I(x, A_4, B_4)) - p\delta) B_4 ds \right| + b|M_4(0) - N_4| \\
 &\leq x_h \theta (r + p\delta_a^{**})C(\epsilon) + \theta(x_e(1 - p)\delta_a^{**} + a)K.
 \end{aligned}$$

By (A.13), we conclude that (iii) holds. □

**Proof of Theorem 3.7** Define a nonlinear mapping  $G : \mathbb{R}^+ \times \mathbb{R}^2 \times X_3 \times X_2 \rightarrow \mathbb{R}^2 \times Y^2 \times \mathbb{R}^3$  by

$$G(\delta, A, N, B, M) = \begin{pmatrix} \left( rf(N) \frac{1}{x_e} \int_{-x_e}^0 g(I(x, A)) dx - \delta - \frac{a}{x_e} \right) A \\ \frac{b}{x_e} (M(0) - N) + \theta \left( p\delta - rf(N) \frac{1}{x_e} \int_{-x_e}^0 g(I(x, A)) dx \right) A \\ D_b B'' - vB' + rBf(M)g(I(x, A, B)) - \delta B \\ D_m M'' + \theta (p\delta - rf(M)g(I(x, A, B))) B \\ D_b B'(0) - vB(0) + aA \\ D_m M'(0) - b(M(0) - N) \\ M(x_h) - M_b \end{pmatrix}, \tag{A.22}$$

where  $X_3 := \{u \in C^2([0, x_h]) : D_b u'(x_h) - vu(x_h) = 0\}$ , and  $X_2, Y$  are defined in (3.13). It follows that  $G(\delta, 0, M_b, 0, M_b) = 0$ . Let  $L := G_{(A,N,B,M)}(\delta_a^*, 0, M_b, 0, M_b)$  be the Frechét derivative of  $G$  with respect to  $(A, N, B, M)$ . For any  $(\xi, \zeta, \varphi, \psi) \in \mathbb{R}^2 \times X_3 \times X_2$ , we have

$$L[\xi, \zeta, \varphi, \psi] = \begin{pmatrix} 0 \\ -\theta \left( (1 - p)\delta_a^* + \frac{a}{x_e} \right) \xi - \frac{b}{x_e} \zeta + \frac{b}{x_e} \psi(0) \\ D_b \varphi''(x) - v\varphi'(x) + (rf(M_b)g(I(x, 0, 0)) - \delta_a^*)\varphi \\ D_m \psi''(x) + \theta (p\delta_a^* - rf(M_b)g(I(x, 0, 0)))\varphi \\ D_b \varphi'(0) - v\varphi(0) + a\xi \\ D_m \psi'(0) - b(\psi(0) - \zeta) \\ \psi(x_h) \end{pmatrix}.$$

If  $(\xi_1, \zeta_1, \varphi_1, \psi_1) \in \ker L$ , then

$$\begin{aligned}
 &-\theta \left( (1 - p)\delta_a^* + \frac{a}{x_e} \right) \xi_1 - \frac{b}{x_e} \zeta_1 + \frac{b}{x_e} \psi_1(0) = 0, \\
 &D_b \varphi_1''(x) - v\varphi_1'(x) + (rf(M_b)g(I(x, 0, 0)) - \delta_a^*)\varphi_1 = 0, \quad 0 < x < x_h, \tag{A.23} \\
 &D_m \psi_1''(x) + \theta (p\delta_a^* - rf(M_b)g(I(x, 0, 0)))\varphi_1 = 0, \quad 0 < x < x_h, \\
 &D_b \varphi_1'(0) - v\varphi_1(0) + a\xi_1 = 0, \quad D_m \psi_1'(0) - b(\psi_1(0) - \zeta_1) = 0, \quad \psi_1(x_h) = 0.
 \end{aligned}$$

Let  $\xi_1 = 1$ . Then, from Lemma A.3,  $\varphi_1 = \hat{\varphi} > 0$  can be uniquely solved, so are  $\zeta_1 = \hat{\zeta}$  and  $\psi_1 = \hat{\psi}$ . Similar to those in the proof of (i) in Theorem 3.5, we have  $\hat{\psi} \leq 0$  and  $\hat{\zeta} < 0$ . If  $\xi_1 = 0$ , we can conclude that  $\varphi_1 \equiv 0$  as  $\delta_* < \delta_a^*$  and consequently  $\zeta_1 = \psi_1 = 0$ . Hence,  $\dim \ker L = 1$  and  $\ker L = \text{span}\{(1, \hat{\zeta}, \hat{\varphi}, \hat{\psi})\}$ . It is also easy to observe that  $\text{codim range } L = 1$  as

$$\text{range } L = \left\{ (\rho_1, \rho_2, \rho_3, \rho_4, \rho_5, \rho_6, \rho_7) \in \mathbb{R}^2 \times Y^2 \times \mathbb{R}^3 : \rho_1 = 0 \right\},$$

and

$$G_{\delta(A,N,B,M)}(\delta_a^*, 0, M_b, 0, M_b)(1, \hat{\zeta}, \hat{\varphi}, \hat{\psi}) = (-1, \theta p, -\hat{\varphi}, \theta p \hat{\varphi}, 0, 0, 0) \notin \text{range } L.$$

By applying Theorem 1.7 in Crandall and Rabinowitz (1971), there exists a positive constant  $\varepsilon_4 > 0$  such that all solutions of (3.14) near  $(\delta_*, M_b, 0, M_b)$  lie on a smooth curve

$$\Gamma_4 = \{(\delta_4(s), A_4^*(s), N_4^*(s), B_4^*(s, x), M_4^*(s, x)) : 0 < s < \varepsilon_4\}$$

with the form

$$\begin{cases} A_4^*(s) = s + o(s^2), & N_4^*(s) = M_b + s\hat{\zeta} + o(s^2), \\ B_4^*(s, x) = s\hat{\varphi}(x) + o(s^2), & M_4^*(s, x) = M_b + s\hat{\psi}(x) + o(s^2). \end{cases} \tag{A.24}$$

Again the direction of bifurcation can be calculated by

$$\begin{aligned} \delta_4'(0) &= - \frac{\langle \hat{l}, G_{(A,N,B,M)(A,N,B,M)}(\delta_a^*, 0, M_b, 0, M_b)[1, \hat{\zeta}, \hat{\varphi}, \hat{\psi}]^2 \rangle}{2 \langle \hat{l}, G_{\delta(A,N,B,M)}(\delta_a^*, 0, M_b, 0, M_b)[1, \hat{\zeta}, \hat{\varphi}, \hat{\psi}] \rangle} \\ &= - \frac{r\gamma_2\mu(0)M_b}{M_b + \gamma_1} + \frac{r\gamma_1\hat{\zeta}}{(M_b + \gamma_1)^2} \frac{1}{x_e} \int_{-x_e}^0 g(I(x, 0))dx < 0 \end{aligned}$$

where  $\hat{l}$  is a linear functional on  $\mathbb{R}^2 \times Y^2 \times \mathbb{R}^3$  defined as  $\langle \hat{l}, (\rho_1, \rho_2, \rho_3, \rho_4, \rho_5, \rho_6, \rho_7) \rangle = \rho_1$  and  $\mu(0)$  can be found in (A.8). This shows that the bifurcation at  $(\delta_a^*, 0, M_b, 0, M_b)$  is backward. This proves part (iii). The proof of part (i) and (ii) is similar to the one for Theorem 3.5, so we omit it here.  $\square$

### Appendix B

We briefly describe the numerical algorithm used in the paper. Divide the interval  $[0, x_h]$  to  $n$  equal size subintervals  $[x^i, x^{i+1}]$ ,  $i = 1, 2, \dots, n, n + 1$  with  $x^i = x^{i-1} + \Delta x$ ,  $x^1 = 0$  and  $\Delta x = x_h/n$  (grid size). We also denote the step size (in the time direction) by  $\Delta t$ . Let

$$u_j^i = u(x^i, t_j), \quad t_j = t_{j-1} + \Delta t, \quad x^i = x^{i-1} + \Delta x, \quad 1 \leq j \leq m, \quad 1 \leq i \leq n + 1.$$

We also define  $u_j^0$  to be the value at  $x^0 = -\Delta x$  and  $u_j^{n+2}$  to be the value at  $x^{n+2} = x_h + \Delta x$ . We use backward differences and central differences as

$$u_t(x^i, t_j) = \frac{u_j^i - u_j^{i-1}}{\Delta t}, \quad u_x(x^i, t_j) = \frac{u_j^i - u_j^{i-1}}{\Delta x}, \quad u_{xx}(x^i, t_j) = \frac{u_j^{i+1} - 2u_j^i + u_j^{i-1}}{(\Delta x)^2}.$$

Then, model (2.1) becomes

$$\begin{aligned} \frac{A_j - A_{j-1}}{\Delta t} &= r A_j f(N_j) \frac{1}{x_e} \int_{-x_e}^0 g(I(x, A_j)) dx - \frac{a}{x_e} A_j - \delta A_j, \\ \frac{N_j - N_{j-1}}{\Delta t} &= \frac{b}{x_e} (M_j^1 - N_j) + \theta p \delta A_j - \theta r A_j f(N_j) \frac{1}{x_e} \int_{-x_e}^0 g(I(x, A_j)) dx, \\ \frac{B_j^i - B_{j-1}^i}{\Delta t} &= D_b \frac{B_j^{i+1} - 2B_j^i + B_j^{i-1}}{(\Delta x)^2} - v \frac{B_j^i - B_j^{i-1}}{\Delta x} \\ &\quad + r B_j^i f(M_j^i) g(I(x^i, A_j, B_j^i)) - \delta B_j^i, \\ \frac{M_j^i - M_{j-1}^i}{\Delta t} &= D_m \frac{M_j^{i+1} - 2M_j^i + M_j^{i-1}}{(\Delta x)^2} + \theta p \delta B_j^i - \theta r B_j^i f(M_j^i) g(I(x^i, A_j, B_j^i)), \\ D_b \frac{B_j^1 - B_j^0}{\Delta x} - v B_j^1 &= -a A_j, \quad D_b \frac{B_j^{n+2} - B_j^{n+1}}{\Delta x} - v B_j^{n+1} = 0, \\ D_m \frac{M_j^1 - M_j^0}{\Delta x} &= b (M_j^1 - N_j), \quad D_m \frac{M_j^{n+2} - M_j^{n+1}}{\Delta x} = M_b, \\ \frac{1}{x_e} \int_{-x_e}^0 g(I(x, A_j)) dx &= \frac{1}{x_e (K_{bg} + l A_j)} \ln \frac{I_{in} + \gamma_2}{I_{in} \exp(-x_e (K_{bg} + l A_j)) + \gamma_2}, \\ I(x^i, A_j, B_j^i) &= I_{in} \exp \left( -K_{bg} (x^i + x_e) - x_e l A_j - l \sum_{k=0}^i B_j^k \right), \end{aligned}$$

for  $1 \leq j \leq m$ ,  $1 \leq i \leq n + 1$ . The simulations in the paper are based on the above numerical algorithm and are implemented in MATLAB.

### References

Alijani, M.K., Wang, H., Elser, J.J.: Modeling the bacterial contribution to planktonic community respiration in the regulation of solar energy and nutrient availability. *Ecol. Complex.* **23**, 25–33 (2015)

Boehrer, B., Schultze, M.: Stratification of lakes. *Rev. Geophys.* **46**, 2 (2008)

Crandall, M.G., Rabinowitz, P.H.: Bifurcation from simple eigenvalues. *J. Funct. Anal.* **8**(2), 321–340 (1971)

Cusseddu, D., Edelstein-Keshet, L., Mackenzie, J.A., Portet, S., Madzvamuse, A.: A coupled bulk-surface model for cell polarisation. *J. Theor. Biol.* **481**, 119–135 (2019)

Du, Y.H., Hsu, S.B.: Concentration phenomena in a nonlocal quasi-linear problem modelling phytoplankton. I. Existence. *SIAM J. Math. Anal.* **40**(4), 1419–1440 (2008)

Du, Y.H., Hsu, S.B.: Concentration phenomena in a nonlocal quasi-linear problem modelling phytoplankton. II. Limiting profile. *SIAM J. Math. Anal.* **40**(4), 1441–1470 (2008)

- Du, Y.H., Hsu, S.B.: On a nonlocal reaction–diffusion problem arising from the modeling of phytoplankton growth. *SIAM J. Math. Anal.* **42**(3), 1305–1333 (2010)
- Edwards, A.M., Brindley, J.: Zooplankton mortality and the dynamical behaviour of plankton population models. *Bull. Math. Biol.* **61**(2), 303–339 (1999)
- Etemad-Shahidi, A., Imberger, J.: Anatomy of turbulence in thermally stratified lakes. *Limnol. Oceanogr.* **46**(5), 1158–1170 (2001)
- Gomez, D., Ward, M.J., Wei, J.C.: The linear stability of symmetric spike patterns for a bulk-membrane coupled Gierer–Meinhardt model. *SIAM J. Appl. Dyn. Syst.* **18**(2), 729–768 (2019)
- Grover, J.P.: Sink or swim? Vertical movement and nutrient storage in phytoplankton. *J. Theor. Biol.* **432**, 38–48 (2017)
- Heggerud, C.M., Wang, H., Lewis, M.A.: Transient dynamics of a stoichiometric cyanobacteria model via multiple-scale analysis. *SIAM J. Appl. Math.* **80**(3), 1223–1246 (2020)
- Henry, D.: Geometric theory of semilinear parabolic equations. *Lecture Notes in Mathematics*, vol. 840. Springer-Verlag, Berlin-New York (1981)
- Hsu, S.B., Lou, Y.: Single phytoplankton species growth with light and advection in a water column. *SIAM J. Appl. Math.* **70**(8), 2942–2974 (2010)
- Hsu, S.B., Wang, F.B., Zhao, X.Q.: Global dynamics of zooplankton and harmful algae in flowing habitats. *J. Differ. Equ.* **255**(3), 265–297 (2013)
- Huisman, J., Weissing, F.J.: Light-limited growth and competition for light in well-mixed aquatic environments: an elementary mode. *Ecology* **75**(2), 507–520 (1994)
- Huisman, J., Arrayás, M., Ebert, U., Sommeijer, B.: How do sinking phytoplankton species manage to persist? *Am. Nat.* **159**(3), 245–254 (2002)
- Huisman, J., Arrayás, M., Ebert, U., Sommeijer, B.: Reduced mixing generates oscillations and chaos in the oceanic deep chlorophyll maximum. *Nature* **439**(7074), 322 (2006)
- Jäger, C.G., Diehl, S.: Resource competition across habitat boundaries: asymmetric interactions between benthic and pelagic producers. *Ecol. Monogr.* **84**(2), 287–302 (2014)
- Jäger, C.G., Diehl, S., Emans, M.: Physical determinants of phytoplankton production, algal stoichiometry, and vertical nutrient fluxes. *Am. Nat.* **175**(4), 91–104 (2010)
- Jiang, J., Shen, A., Wang, H., Yuan, S.L.: Regulation of phosphate uptake kinetics in the bloom-forming dinoflagellates *Prorocentrum donghaiense* with emphasis on two-stage dynamic process. *J. Theor. Biol.* **463**, 12–21 (2019)
- Jiang, D.H., Lam, K.Y., Lou, Y., Wang, Z.C.: Monotonicity and global dynamics of a nonlocal two-species phytoplankton model. *SIAM J. Appl. Math.* **79**(2), 716–742 (2019)
- Klausmeier, C.A., Litchman, E.: Algal games: the vertical distribution of phytoplankton in poorly mixed water columns. *Limnol. Oceanogr.* **46**(8), 1998–2007 (2001)
- Liu, P., Shi, J.P., Wang, Y.W.: Imperfect transcritical and pitchfork bifurcations. *J. Funct. Anal.* **251**(2), 573–600 (2007)
- Loladze, I., Kuang, Y., Elser, J.J.: Stoichiometry in producer–grazer systems: linking energy flow with element cycling. *Bull. Math. Biol.* **62**(6), 1137–1162 (2000)
- Lv, D.Y., Fan, M., Kang, Y., Blanco, K.: Modeling refuge effect of submerged macrophytes in lake system. *Bull. Math. Biol.* **78**(4), 662–694 (2016)
- Mei, L.F., Zhang, X.Y.: On a nonlocal reaction–diffusion–advection system modeling phytoplankton growth with light and nutrients. *Discrete Contin. Dyn. Syst. Ser. B* **17**(1), 221–243 (2012)
- Mei, L.F., Zhang, X.Y.: Existence and nonexistence of positive steady states in multi-species phytoplankton dynamics. *J. Differ. Equ.* **253**(7), 2025–2063 (2012)
- Mischaikow, K., Smith, H., Thieme, H.R.: Asymptotically autonomous semiflows: chain recurrence and Lyapunov functions. *Trans. Am. Math. Soc.* **347**(5), 1669–1685 (1995)
- Nie, H., Hsu, S.B., Wang, F.B.: Steady-state solutions of a reaction–diffusion system arising from intraguild predation and internal storage. *J. Differ. Equ.* **266**(12), 8459–8491 (2019)
- Nishimura, Y., Kim, C., Nagata, T.: Vertical and seasonal variations of bacterioplankton subgroups with different nucleic acid contents: possible regulation by phosphorus. *Appl. Environ. Microbiol.* **71**(10), 5828–5836 (2005)
- Pao, C.V.: *Nonlinear Parabolic and Elliptic Equations*. Plenum Press, New York (1992)
- Paquin-Lefebvre, F., Xu, B., DiPietro, K.L., Lindsay, A.E., Jilkine, A.: Pattern formation in a coupled membrane–bulk reaction–diffusion model for intracellular polarization and oscillations. *J. Theor. Biol.* **497**(110242), 23 (2020)

- Paquin-Lefebvre, F., Nagata, W., Ward, M.J.: Weakly nonlinear theory for oscillatory dynamics in a one-dimensional PDE-ODE model of membrane dynamics coupled by a bulk diffusion field. *SIAM J. Appl. Math.* **80**(3), 1520–1545 (2020)
- Peng, R., Zhao, X.Q.: A nonlocal and periodic reaction–diffusion–advection model of a single phytoplankton species. *J. Math. Biol.* **72**(3), 755–791 (2016)
- Ryabov, A.B., Rudolf, L., Blasius, B.: Vertical distribution and composition of phytoplankton under the influence of an upper mixed layer. *J. Theor. Biol.* **263**(1), 120–133 (2010)
- Shi, J.P., Wang, X.F.: On global bifurcation for quasilinear elliptic systems on bounded domains. *J. Differ. Equ.* **246**(7), 2788–2812 (2009)
- Song, D., Fan, M., Chen, M., Wang, H.: Dynamics of a periodic stoichiometric model with application in predicting and controlling algal bloom in Bohai Sea off China. *Math. Biosci. Eng.* **16**(1), 119–138 (2019)
- Vasconcelos, F.R., Diehl, S., Rodríguez, P., Hedström, P., Karlsson, J., Byström, P.: Asymmetrical competition between aquatic primary producers in a warmer and browner world. *Ecology* **97**(10), 2580–2592 (2016)
- Wang, H., Smith, H.L., Kuang, Y., Elser, J.J.: Dynamics of stoichiometric bacteria–algae interactions in the epilimnion. *SIAM J. Appl. Math.* **68**(2), 503–522 (2007)
- Wang, F.B., Hsu, S.B., Zhao, X.Q.: A reaction–diffusion–advection model of harmful algae growth with toxin degradation. *J. Differ. Equ.* **259**(7), 3178–3201 (2015)
- Wang, Y., Shi, J.P., Wang, J.F.: Persistence and extinction of population in reaction–diffusion–advection model with strong allee effect growth. *J. Math. Biol.* **78**(7), 2093–2140 (2019)
- Wüest, A., Lorke, A.: Small-scale hydrodynamics in lakes. *Annu. Rev. Fluid Mech.* **35**(1), 373–412 (2003)
- Yoshiyama, K., Nakajima, H.: Catastrophic transition in vertical distributions of phytoplankton: alternative equilibria in a water column. *J. Theor. Biol.* **216**(4), 397–408 (2002)
- Yoshiyama, K., Mellard, J.P., Litchman, E., Klausmeier, C.A.: Phytoplankton competition for nutrients and light in a stratified water column. *Am. Nat.* **174**(2), 190–203 (2009)
- Zagaris, A., Doelman, A.: Emergence of steady and oscillatory localized structures in a phytoplankton–nutrient model. *Nonlinearity* **24**(12), 3437–3486 (2011)
- Zhang, J.M., Shi, J.P., Chang, X.Y.: A mathematical model of algae growth in a pelagic–benthic coupled shallow aquatic ecosystem. *J. Math. Biol.* **76**(5), 1159–1193 (2018)

**Publisher's Note** Springer Nature remains neutral with regard to jurisdictional claims in published maps and institutional affiliations.